Simulation and Economic Analysis of Parabolic Trough Solar Assisted Single Effect Absorption Chiller for Famagusta, Cyprus

Reyhaneh Jabbari Sahebari

Submitted to the
Institute of Graduate Studies and Research
in partial fulfillment of the requirements for the degree of

Master of Science
in
Mechanical Engineering

Eastern Mediterranean University
February 2017
Gazimağusa, North Cyprus

Approval of the Institute of Graduate Studies and Research

Prof. Dr. Mustafa Tümer
Director

I certify that this thesis satisfies the requirements as a thesis for the degree of Master of Science in Mechanical Engineering.

Assoc. Prof. Dr. Hasan Hacışevki
Chair, Department of Mechanical Engineering

We certify that we have read this thesis and that in our opinion it is fully adequate in scope and quality as a thesis for the degree of Master of Science in Mechanical Engineering.

Prof. Dr. Uğur Atikol
Supervisor

Examining Committee

1. Prof. Dr. Uğur Atikol

2. Prof. Dr. Fuat Egelioğlu

3. Dr. Devrim Aydin

ABSTRACT

This research contemplates on the valuable utilization of solar based energy intended for a restricted region in the Mediterranean basin. Especially in Mediterranean section with high solar gains and high cooling demands, solar cooling will become more and more an alternative to established cooling systems. Solar energy turns out to be progressively well-known and the accessible solar oriented market is explored with the point of selecting and evaluating a pilot locale for a promising solar based application. The system is displayed and assessed in details for the authentic related analysis application.

The goal of this study is to access the traces of using underground water temperature instead of the inlet temperature of condenser on the energy outputs of the generator, the condenser and the evaporator, moreover, to investigate the feasibility of a solar single lithium bromide-water absorption cooling system for Famagusta, Cyprus. The system has been intended to supply cooling loads of the office building area of approximately 200 m² for working hours from 9 am to 16 pm, 5 days a week, in all hot weather states of Famagusta. TRNSYS software program has been used to estimate the performance of the system throughout the summer season. The performance calculations indicate that:

- A 35kW absorption chiller is sufficient to appropriate the 200 m^2 office space cooling requirements,
- Use of 30 m^2 parabolic trough collectors will be sufficient to operate the absorption chiller,

- 22℃ underground water is better to use in condenser and absorber instead of cooling tower water, which is commonly used in industries that provides a minimum sink temperature of 32℃,
- COP of the system is obtained as 0.672 for 22℃ of the condenser inlet temperature of underground water.

Keywords: solar absorption cooling system, parabolic trough solar collector, Cyprus climate conditions, life cycle cost analysis

ÖZ

Bu araştırma, Akdeniz havzasındaki sınırlı bir bölgeye yönelik güneş enerjisine dayalı enerjinin değerli kullanımı üzerinde düşünülmektedir. Özellikle Akdeniz bölümünde yüksek güneş enerjisi kazanımı ve yüksek soğutma ihtiyacı ile güneş soğutması, kurulan soğutma sistemlerine göre daha fazla seçilen seçenek olacaktır. Güneş enerjisi (solar enerji) aşamalı olarak uygulanarak bilinir ve erişilebilir olan güneş odaklı uygulama pazarı, umut verici bir şekilde güneş temelli uygulama için bir pilot yerleşim seçimi ve değerlendirmesi noktasında kurularak araştırılır. Sistem, gerçek ve güvenilirlikle ilgili analiz uygulaması için ayrıntılı olarak görüntülenir ve değerlendirilir. Bu yazının amacı, jeneratörün enerji çıkışlarındaki yoğunlaşmanın giriş sıcaklığı yerine yeraltı suyu sıcaklığı kullanma izlerini tahmin etmektir. Kondansatör ve buharlaştırıcı, Gazimağusa Kıbrıs için güneşi kullanarak tekli lityum bromür su soğurma ve soğutma sisteminin fizibilitesini sürükleyecektir (sürdürülebilecektir). Sistem, çalışma saatleri için sabah 09: 00'dan 16: 00'a kadar yaklaşık 200 m² ‘lik bir ofis binası alanının soğutma yüklerini tedarik etmeyi amaçlamıştır. Sistem modeli parabolik Geçiş (sürgü) toplayıcıları; sıcak bir depoda, bir LiBr-water ‘lik emici soğutucu ve fan soğutucu entegre sayılarını hariç tutmuştur. Performans ve maliyet üzerindeki etkiler gözden geçirilmiştir. Performans hesaplamaları sonucu şu bulgulara varılıyor:

- 35kW emici bir soğutucu, 200 m² ofis alanı soğutma gereksinimlerini karşılamak için yeterlidir.
- Soğutucunun çalışmasını isteyen 30 m² 'lik toplayıcılardır.

- 22 ℃'deki yer altı suyu, yoğunlaştırıcı ve soğurucuda çalişmasi için soğutma kulesi yerine ki minimum su sıcaklığı yaklaşık 32 ℃'dir, daha iyi kullanılır.
- Kondansatör giriş soğutma suyu sıcaklığı 22 ° C için, soğutma çevriminin etkinlik kat sayısı (COP) 0.672 elde edilmiştir.

Anahtar kelimeler: güneş enerjisi soğutma sistemi, parabolik oluk tipi güneş kolektörü, Kıbrıs iklim koşulları, yaşam döngüsü maliyet analizi

To my lovely Family; my Dad, Mom and my sweetie Sister.

I love you so much, I just live for you.

Always be with me.

ACKNOWLEDGEMENT

I would first like to declare my sincere appreciation to my thesis supervisor Prof. Dr. Uğur Atikol representing his leadership, patience, assurance and advices throughout the whole progress of this thesis review, preserve me profitable.

I would like to thank my great family instead of their supports and reliefs during my life with fortitude and love. The love of family is a exquisite reward which I touch honoured and blessed to carry. A special thanks to all my family and friends who have been comprehending and caring all over this effort, rowelling me on with persuasion and appears of love.

A special thanks to my friends Cihan Şahin, Hamed Pourasl, Sara Rezai, Hamed Ghasemiyan and Vahid Khojasteh, for their friendship and assists throughout the master program. I feel really lucky to have the great friends as a big family like you.

Finally, and most significantly, I wish to state my truthful gratitude for my sister, Tara Jabbari.s. Her morale and complete faith in my aptitude to surpass in this job was an primary point of my success. Furthermore, her concerns on me as well as her delicious foods are unforgettable events.

TABLE OF CONTENTS

LIST OF TABLES

LIST OF FIGURES

LIST OF SYMBOLS

Notation and Units

A	Total available heat exchange surface area (m^2)
c	Specific heat capacity ($kJ/kg.K$)
C	Capital cost ($)
COP	Coefficient of performance
E	Effectiveness (%)
H	Specific enthalpy (kJ/kg)
ΔH	Enthalpy change (kJ)
I	Radiation ($kJ/hr.\ m^2$)
i	Interest rate (%)
K	Thermal conductivity (W/mK)
L	Length (m)
LCC	Life cycle cost ($)
M	Mass (kg)
$\dot{m}$	Mass flow rate (kg/s)
P	Power (W)
p	Pressure (Pa)
Q	Rate of heat transfer (kW)
R	Thermal resistance ($m^2.K/W$)
r	Discount rate (%)
R_b	Slope factor
T	Temperature ($℃$)
ΔT	Temperature difference ($℃$)

$T_{s,i}$	Saturation temperature (℃)
TRNSYS	TRaNsient SYstem Simulation program
U	Overall heat transfer coefficient ($kW/m^2.K$)
V	Volume *(m3)*
v	Specific volume (m^3/kg)
W	Work (kW)
w	Width (m)
X	Concentration of aqueous LiBr solution (%)
x	Thickness *(mm)*
ρ	Density (kg/m^3)
η_{th}	Thermal efficiency

Subscripts

a	Absorber
c	Condenser
chill	Chilled stream
cool	Cooling stream
e	Evaporator
g	Generator
hot	Hot stream
HX	Heat exchanger
i	inside
l	liquid
n	Index (1,2,…)
o	outside
p	Pump
r	Refrigerant
s	Aqueous LiBr solution rich in refrigerant (strong solution)
SAC	Solar Absorption Chiller
sat	Saturated condition/saturated state
SHX	Solution Heat Exchanger
sol	Aqueous LiBr solution
v	vapor
w	water

Abbreviations

ACS	Absorption Cooling System
CPC	Compound Parabolic Collector
ETC	Evacuated Tube Collector
FLC	Frensnel Linear Collector
FPC	Flat Plate Collector
H_2O	Water
IRR	Internal Rate of Return (%)
LiBr	Lithium Bromi
NPV	Net Present Value
PBP	PayBack Period
PTC	Parabolic Trough Collector
PV	Photo Voltaic
SACS	Solar Absorption Cooling System
SCS	Solar Cooling System
SIR	Saving to Investment Ratio (%)
SPP	Simple Payback Period

Chapter 1

INTRODUCTION

1.1 Background

Cyprus has a passionate Mediterranean situation with the distinctive seasonal sequence intensely specified in characteristic of temperature, rainfall and weather. Hot days of summer are ranged from the middle of the May to mid-September in Cyprus weather settings. For the most parts, warm temperature season keeps going around eight months. It starts in April through average temperature of 21 to 23 °C up to the November by average temperature of 22 to 23 °C. The middle of summer (July and August) is generally hot, with an average maximum coastal temperature of around 33 °C during the day [1].

The temperature goes up to 45 °C in summer. In view of the climate conditions around the Mediterranean ocean and on islands, the buildings are warming up and in order to this case cooling is the premier task of building thermal energy system. The world air conditioning energy demand supplement is endlessly increasing. Electrically powered are the conventional cooling units are the top interest of electricity in summer increments and enhances the content limit in Cyprus. Since a large portion of the electricity originates from fossil sourced power plants, it expands the generation of Carbon dioxide.

The electricity consumption increments in summer season due to the expanded cooling demand for covering the thermal solace conditions in buildings. Vapor compression air conditioning systems are generally utilized to maintain the cooling demand due to their low purchase costs furthermore, accessible operation essences when contrasted with other different air conditioners. The compressor expends too much electricity in vapor compression devices. This indicates the need for reduction of essential energy utilization and the abatement of the worldwide cautioning effect of HVAC systems. Hence, study is fundamental with a specific end goal to diminish the expense of utilizing solar based air conditioning as a part of structures.

The Coefficient of Performance (COP) of the absorption coolers are suggestively lower than conventional chiller. Single effect absorption chillers offer the COPs of 0.65 to 0.7 and double-stage absorption chillers can accomplish COPs of approximately 1.2 and triple effect types have calculated COPs from 1.4 to 1.6 [2]. The heat temperature is the extremely critical factor in the thermal effectiveness of an absorption cooling system. COP of the system is increasing via the decline of heat sink temperature. Underground water can be considered a potential source of energy let us turn to the condenser, one of the components of absorption chiller and see how it helps to increase the COP of devise. The cooling towers are commonly used in industries to reject heat through the natural process of evaporation. But the relative humidity of air in Cyprus at summer is so high therefore the cooling tower will not be able to extract more process and will not run at a cooling temperature because the humid air has not a great capacity to absorb the warm water.

The ambient temperature in Cyprus is approximately from 40 to 45 ℃ at hot summer day but the temperature of underground water in Famagusta is 22 ℃ whole summer.

The water temperature in the closed water source as condenser must be maintained within a narrow degree range for obtaining a steady system performance. Therefore, underground water is potentially an effective source required in this component of absorption chiller to increase the COP of single effect absorption chiller.

1.2 Scope and Objectives

The aim of this research is to estimate a feasibility of a solar absorption chiller utilizing ground water as heat sink according to Cyprus weather conditions. A solar absorption chiller consisting of parabolic trough solar collector, storage tank and a single-effect LiBr-water absorption chiller that will insurance a representative office building load for the period of the entire year. The working pairs utilized in the absorption chiller is LiBr-water. In some areas of Famagusta, the sea water has penetrated under the ground which has a temperature of 18-22 ℃, for that reason it seems suitable to use underground water as heat sink to reject heat thereby to drive the condenser component in absorption chiller.

The dynamic performance in terms of the condenser water cooling temperature rise, the rate of energy gained and the coefficient of performance for the absorption chiller has been researched hypothetically through the TRNSYS simulation program. Additionally, the influence of the cooling capacity and the collector aperture area at the operating period of the solar absorption cooling system has been explored in this research.

The impacts on accomplishment and on costs have been investigated for office building performing states. Financial analysis of solar sourced single effect absorption cooling systems has been explored.

The scopes of this thesis are;

- to evaluate the vitality request of the respect buildings by utilizing demonstrating tools for this reason.
- to display a strategy to approve an absorption machine (for the HVAC system), as an approach to rise the general efficiency of the building.

The objectives of the research are:

- to improve solar absorption cooling arrangement through of system simulation. There are broad reviews on solar absorption cooling systems which use cooling tower and thus, the condenser temperature is restricted in the range of 25℃ to 30℃. The underground water expands the cost of the system and has a huge system volume. In this study, a programming model is simulated for LiBr/Water absorption system with underground sea water sourced condenser and absorber to be utilized as a part of remote territories with restricted access to electricity.
- to give a far reaching seeing how different inlet cooling water temperatures, affect the energy balance and system COP.
- to evaluate the modelling results by evaluating the outcomes from TRNSYS program and the possible reasons.
- to bring forward how the inactive (solar collectors) and active (absorption chiller) extents which may be existed, are chipping in enhancing the energy utilization in the building.

- to determine the validity of the system by detecting the effects of the unit prices, load factor of the system, internal rate of return (IRR), net present value.
- To analyse the net present value, payback period and saving to investment ratio for determination of the feasibility of the system.

1.3 Geographical and Climate Features

North Cyprus as well as the whole island enjoys typical Mediterranean climate with long, warm and dry summers from mid-May to mid-October and mild and wet winters from December to February. The short autumn and spring periods complete the seasons of the year.

Cyprus contains warm and inclement winter that is started since December to March, as well as hot along with dry summer that is ranged as of June to mid-October, which is difined as Mediterranean weather.

Summer in Northern Cyprus is a season of hot weather, high temperatures and cloudless sky, but the sea breeze make a pleasant atmosphere in coastal areas. The temperature of the hottest months of July and August crawls to 34 °C and even to 40 °C. Cyprus receives an average of 2,700 to 3,500 hours per year. The survey on monthly total of sun hours over the year in Famagusta, displays that, July involves the maximum sunny days of the year. the average sunny hours a month in July is approximately 400 hours a month. The maximum humidity is 75% at January and the minimum average humidity at summer season is approximately 55% at June [3].

The meteorological conditions odata format of Larnaca is used in the simulations as it is the only accessible Cyprus location in Energy Plus database. Significant daily

and seasonal variances surrounded by sea and inland are stimulated via high sunshine rate and clear sky. It commands through resident influences by the sea. There is approximately 5 hours of sunshine each day in winter and it is greater to 12 hours for the period of the summer. Average of 5.5 hours a day sunshine appears in cloudiest months, though, this rate rising up to 11.5 hours of sunny each day in summer [4].

1.4 Outline

Very well characterized system setup is needed to simulate the solar absorption chiller to be utilized in office building. The first Chapter is explained the introduction and scope and objectives of the study even it gives the information about the geographical and climate features about Famagusta, Cyprus. The second Chapter presents the literature review that contains a diagram of the reviews found in the literature on passive cooling techniques and solar sourced absorption systems. The requirement of these researches to advance the assumption of solar absorption cooling systems and how it has affected the design of these systems is additionally displayed. Furthermore, the system cost is briefly analysed. Moreover, direct vs indirect and single vs double stage ACSs are compared.

In Chapter 3, a solar absorption system is discussed. The Chapter begins with introduction of absorption cooling systems and examining how it works. The basic components that generally used in the typical solar absorption cooling systems are explained via details likewise the mathematical parameters and equations that explain their execution are given.

Chapter 4 presents TRNSYS simulation software, performed simulation of obtained results in that software. The whole system performance analysis completed on the

solar absorption system and the computed primary execution pointers were also presented.

Chapter 5, renders the system simulation results under various optimal conditions. Meanwhile, discussion of system operation and financial analysis has been executed for the typical office building in Cyprus weather condition. Additionally, contains correlation of results and the system performance data and variations are clarified.

The fundamental conclusions of the presented research review are condensed and the attainments are exhausted in Chapter 6. The results are discussed and afterward future enhancements prescribed.

Chapter 2

LITERATURE REVIEW

There is an enormous amount of papers on solar cooling literature, improve and boost a varied assortment of solar cooling decisions, especially ACS. Mokhtar et al. It represents a surplus that represents an evaluation of solar energy-driven cooling developments in the solar system [5]. Consequences demonstrated which vast measure cooling plant alternatives are the supreme sparing. On a tiny measure, Fresnel concentrators and slight film photovoltaic (PV) cells are financially most flexible technologies. Regarding general proficiency, on the other hand, multi- crystalline PV cells through vapor-compression cooling systems were the greatest proficient alternative of all. Solar asset accessibility is the main consideration in deciding the most appropriate solar cooling innovation for a specific area.

Preferable to reduce the electricity demand in the summer season by absorbing the heat as a chemical compression device that is in violation of the vapor compression. Regarding to energy economy and feasibility, cooling chillers can be set instead of steam compression systems because they consume heat without using electricity. A more inventive way to obtain cooling is to utilize solar energy in a heat powered absorption system for air cooling. The high relationship between the accessibility of solar energy and the requirement for cooling gives an inalienable point of preference to solar powered driven cooling system.

Furthermore, the most important advantage of using absorption systems is exploitation of the refuse heat from generation likewise solar heat. Providing the absorption cooling cycle makes immediate and competent use of solar powered heat, supplanting the utilization of common gas or electric power for compaction refrigeration [6].

Solar collectors and absorption chiller cost are the primary supporters to the aggregate system cost. The impacts of the unit prices of the absorption chiller and solar collectors rely on upon the innovation improvement. In any case, electricity costs increase yearly because of the expanded fuel costs. Otanicar et al. [7] figured out an assortment of solar cooling plots and uncovered some keys insights with respect to the decision of the system considering monetarily and ecologically perspectives: The cost of solar electric cooling system is profoundly subject to the system COP while photovoltaic (PV) costs stay at the present points yet while costs are brought down the effect of COP upon cost declines. The expense of solar collector is greatly lesser identical to rate of the total cost pro solar thermal cooling however the expense of the refrigeration system speaks to a bigger rate of the aggregate expense. Furthermore, the paper uncovers which the expenses instead of solar cooling are not anticipated to diminish as greatly as PV cooling throughout the following 20 years because of the generally constant expense of set and loading.

Absorption cooling devices are adequate to drive directly or indirectly [8]. Indirect ACS consumes heat from renewable energies essentially solar and geothermal energy to the outcome the cooling impact. Direct ACS working with natural gas then applies the outcome heat to ACS units. Directly works ACS alternative relies on the natural gas cost when contrasted with electricity offering cost. Electricity consumption

decreases with the use of renewable energy in indirect -fired ACS, therefore, energy efficiency, and feasibility might be contented. The temperature and mass flow rate of source are essential to settle on the type of an ACS. Adequate source temperature in single effect ACS is approximately 100°C and for double effect ACS, required source temperature is relatively 150°C in the interest of its higher COP. It is credible to utilize a heat recuperation choice furthermore COP can be expanded by utilizing low temperature generators as a part of double effect ACS. The COP value for single effect and double effect ACS is around 0.7 and 1.2 respectively at full load conditions [9].

Florides et al. [10] issued a strategy to assess the qualities and execution of single effect LiBr-water absorption chiller. Single valley vertical tube heat exchangers were utilized for condenser and evaporator. Condenser and generator were considered as flat tube heat exchangers. COP was found 0.704, for 10 kW cooling output. High performance and low cost of the LiBr- water absorption cooling system causes the system be suitable for in air conditioning. The system operates with less energy, subsequently it can utilize renewable energies.

N.K. Ghaddar et al. [11] exhibited a model of solar powered absorption cooling system in Beirut. The outcomes demonstrated that collector area >23.3 m2, coupled with tank with the volume range of 1000-1500 litres is required for each kW of refrigeration for a system to directly work only with solar energy by a round seven hours per day. This suggests the importance of utilizing ACS for reducing global energy for ACS. Absorption chillers are not still dominant to mechanical compression cycles. Hence, study is fundamental with a specific end goal to diminish the technical and economic feasibility of utilizing solar based air conditioning in a part of structures.

Lizarte et al. [12] performed a study on single effect air cooled LiBr/H2O absorption chillier for residential utilization. The model gains an ostensible cooling load of 4.5 kW along with, it was driven by thermal energy generated from 42.2 m vacuum flat plate solar collector. The outcomes demonstrated that the system could generate an average of 3.35 kW of cooling load, over a period of 7.5 h with a mean daily COP of 0.62.

Chemisana et al. [13] presented a comparison between two cooling systems for a specific three-floor building, with and without solar concentration. The first is a conventional system which consists of evacuated tube collectors feeding single-effect absorption chillier. On the other hand, a Fresnel reflective solar concentrating system is coupled to double-effect absorption chillier. The results showed an important reduction of the solar collectors' absorber area in the concentrating system compared with the standard solar thermal installation. However, the solar concentrating system requires a large aperture area. In addition, the rejected heat in the double-effect chillier is lower, implying that the investment and operation costs of the solar concentrating cooling system can be reduced significantly.

Assilzadeh et al. study a solarabsorption system designed for a tropical climate in Malaysia using TRNSYS software [14]. Through a sensitivity analysis by varying the collector area and slope, the storage tank volume, and the pump flow rate, the optimal design of the system for Malaysia's climate was determined for continuous reliable operation of the system.

Blinn et al. [15] have developed a model of TRNSYS full simulation through LiBr/Water absorption cooling cycle to the housing solar absorption cooling system

utilized in southern United States. System performance can enhance by expanding the dead band of the thermostat, recurrence of driving and lessening auxiliary utilization. The solar fraction is most noteworthy at least possible temperature of source for FPCs. Equivalent heat supplementary prompted to a grander solar segment than the series auxiliary. Vapor pressure surrenders higher solar segment than auxiliary and needs lower supplementary power. The temperature of crossing hot water and cooling water are setting by the chiller capacity and COP and is detailed with performance bends holding up by experiments or manufacturers.

Chapter 3

METHODOLOGY

3.1 System Description

The single stage absorption system embraces of four noteworthy sections, i.e., a generator, a condenser, an evaporator and an absorber. These existent factors are separated addicted to three sections via one heat exchanger, two expansion valves and a pump. Schematic diagram of single-effect solar absorption chiller is shown in Figure 1. The offered SACS via this research involves of the combination of the 15kW single stage LiBr-water absorption cooling machine including several Parabolic Trough Solar collectors (PTC). The solar collectors are treated in place of a heat source for heating the water to use in absorption cooling cycle. A hot water-fired storage tank was consumed between the solar collector and the absorption device for keeping up a constant energy input to the cooling machine. A pump is used to transfer the water from the solar collector to the storage tank, stream 1. A typical constant speed pump delivers the heated water from the storage tank to the ACS, stream 4. A pump was used to drive the water in the solar circuit. For maintaining the collector temperature rise $>10\ ^{o}C$ an on/off controller was used. While the temperature of the solar collector is below 10 ^{o}C the controller send a signal to the pump to stop the fluid circulation. When the outlet fluid temperature flowing through storage tank to the absorption chillier is beyond $100^{\circ}C$ the controller forward a signal to circulating pump to circulate the hot fluid to the absorption chillier.

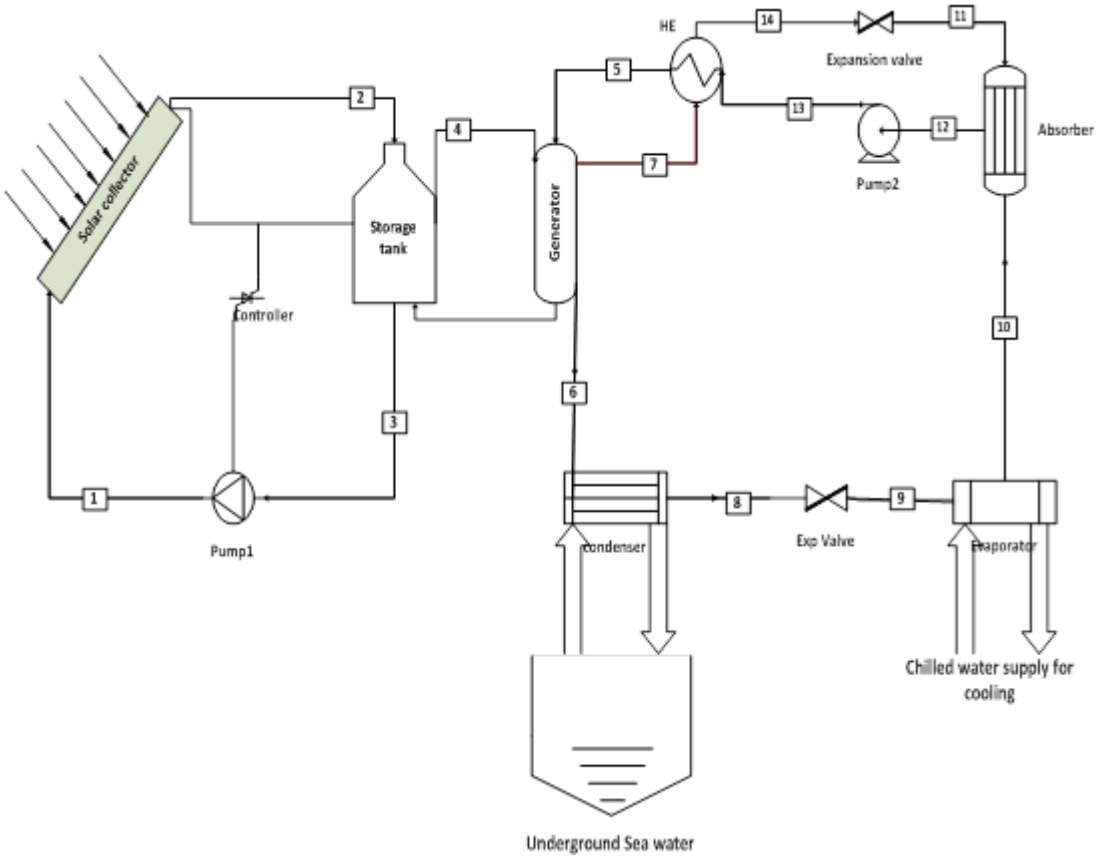

Figure 1: Schematic of Solar Single Effect Absorption System.

The heat derived from the solar collector is isolated by water vapor in the LiBr solution in the generator, stream 4. Condensation of the lithium bromide solution rises at high temperature and pressure. Meanwhile, the water vapor is transferred to the condenser, as shown in Figure 3.1 stream number 6. During this process steam is cooled and is converted to liquid by the heat rejection to underground sea water. After that liquid water at high pressure enters to the expansion valve, stream 8, and then moved to evaporator, stream 9. Here, liquid water is evaporated at low pressure and temperature, while providing cooling effect by absorbing latent heat of evaporation from surroundings. Later on, the water vapor is transferred to the absorber part, stream 10. At the same time, the strong solution of lithium bromide flows to the heat exchanger after leaving the generator, accordingly to heat up the weak suspension retracting the

generator, stream 7. The strong solution then transferred to the absorber where heat is rejected to the environment, stream 11. The water vapor getting out of the evaporator is absorbed by the strong lithium bromide solution in the generator to make a weak solution, stream 12. At the end, the water is pumped again to the generator, stream 5, and the cycle is repeated.

Briefly, the cooling water supplied to the condenser and then the absorber is provided by the underground sea water which has the constant temperature approximately 22℃ in Cyprus in summer conditions, for removing the heat from the system. The impact of the absorber temperature on the system effectiveness is higher than the temperature of the condenser which condensing by the underground water where the heat is decomposed to the space. It is exceedingly prescribed to utilize an apportioned hot water storage tank to work as two apart tanks. The upper part of the tank is attached to the solar collectors at the morning, while whole the tank could be used at the evening to put out the heat energy to the absorption chiller.

Temperature contrast between the generator, condenser and absorber units is administered to a great extent in the performance of the system. Therefore, temperature of the condenser and absorber must be keep in low.

Using LiBr seems more advantages then using ammonia in solar absorption chillers. Because in LiBr based ACS the generator requires lower temperature than the ammonia system. In LiBr-Water absorption chillers, allowable temperature for generator ranges from 76-99℃, while, it is approximately 95-120℃ in water cooled ammonia absorption system [16]. Most of the industrially accessible absorption

chillers utilize LiBr-Water as the refrigerant couple, because of the higher crystallization temperature of the LiBr solution with air cooling, these units must be water cooled.

Various equipment demands and constrains must be decided upon with the investigation and design of solar sourced absorption systems. The primary evaluation includes the sort of collector utilized. Parabolic trough and flat plate collectors could be suitable to capture the temperature needed by absorption chillers.

3.1.1 Solar Powered collectors

Solar collectors are one of the methods for concentrating the sun beams to heat up fluids. Appropriate solar collectors are needed to convey high temperature with great efficiency for generator input. Solar powered collectors are essentially categorized via their movement, i.e. fixed, single axis pursuing and two axes pursuing, and the working temperature. Firstly, the fixed solar collectors are analysed. These collectors are for all time settled in spot, moreover, do not path the sun. Three categories of collectors exist in this classification;

i. Flat plate collectors (FPC);
ii. Compound parabolic collectors (CPC);
iii. Evacuated tube collectors (ETC).

Parabolic Trough Collectors are regularly utilized as a part of dynamic, indirect water heating systems. These types of collectors work great in Cyprus weather conditions where there is a high amount of direct solar radiation and no deficiency of daylight and virtually very low clouds.

These kinds of collectors follow the sun's daily motion to get straight sun based radiation. This collector with horizontal north-south district axis is the extremely routine. Figure 2 [17]. indicates gathering of beam radiation and heat losses of parabolic trough collector. This kind of collector basically comprises of mirroring surface (shaped parabola) that concentrate the rays of the sun on a pipe conveying reasonable fluid such as water.

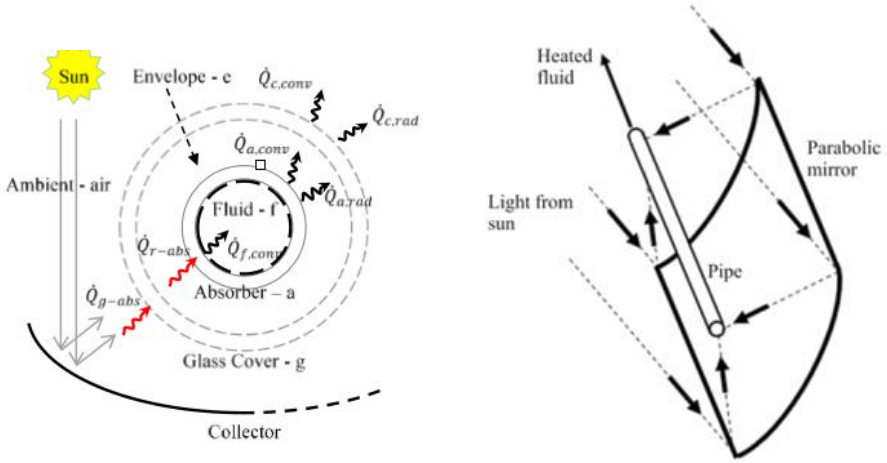

Figure 2: Schematic of the Parabolic Trough Solar collector [17].

Hot water generated via Compound Parabolic collector (CPC) is ranged between 90°C and 110°C, with gathering efficiencies (ratio between thermal power at collector outlet and incident radiation) in the scope of 40%-50%; over this farthest of temperature the efficiency decreasing rapidly to zero [18]. Parabolic Trough (PTC) and Fresnel Linear Collectors (FLC) effortlessly warm up thermal oil or steam at temperatures up to 200°C, very similar transformation efficiencies.

During the circulation of the fluid in the pipe, temperature of the fluid increments as it flows down along the solar collector. The pipe augments the whole length of the reflecting surfaces.

3.1.2 Single Effect Absorption Cooling System

An absorption refrigeration cycle uses the principles of heat transfer and change of phase of the refrigerant to produce the refrigeration effect. The system provides a cooling effect by absorbing heat from one fluid (chilled water) and transferring it to another fluid (cooling water or ambient air). It also uses a device (thermal compressor) to increase the pressure of the refrigerant and an expansion device to maintain the internal pressure difference.

There are two fundamental differences between the absorption cycle and the vapor compression refrigeration (VCR) cycle. First, the mechanical compressor in VCR is replaced by an absorber, pump, and generator (thermal compressor). Second, the absorption refrigeration cycle uses a secondary fluid (absorbent) to carry the refrigerant from the low-pressure side (evaporator) to the high-pressure side (condenser).

Generally, an evaporating refrigerant absorbs by an absorbent, on low-pressure part. The two most common refrigerant/absorbent mixtures used in absorption chillers are lithium bromide water (LiBr-H_2 O) where water vapor is the refrigerant and ammonia-water (NH_3 -H_2 O) systems where ammonia is the refrigerant. In contrast to vapor compression cooling system the essential thought of an absorption cycle is to avoid from compression work. This is finished by utilizing a reasonable working pair. This pair comprises of the refrigerant combined with solution to attract the refrigeran. The ammonia-water couple has some drawbacks with compared to the LiBr cycle for instance;

- The lower coeficient of execution of NH_3 -H_2 O than LiBr-H_2 O. The coeficient of performance of NH_3 -H_2 O is between 0.6 to 0.7, including the charecterized while the amount of the cooling influence to the heat input, whearas, The COP of this system is among 0.6 as well as 0.8 [19].
- The greater inlet temperature needed pro NH_3 -H_2 O than LiBr-H_2 O. Generator inlet temperature required for LiBr-H_2 O ranges from 70℃ to 88℃, whereas NH_3 -H_2 O needs temperatures of 90-180℃.
- It needs higher pumping pressure and thus higher pumping power.

Water is used as the refrigerant, in LiBr-H_2 O system. The LiBr-H_2 O systems have a disadvantage that their evaporator can not be run at temperatures <5°C. There are two types of absorption cooling systems available namely; single stage and double stage.

The single stage ACS is mostly utilized in favour of building cooling contents, in this case chilled water is needed at 6°C to 7°C [20]. The COP will differ to a undersized amount of the heat source temperature and the temperature of cooling water. Single stage ACSs are able to work among hot water temperature in the range of 80°C to 150°C whilst water is pressurised [21]. The schematic diagram of the single stage ACS is shown in Figure 3.

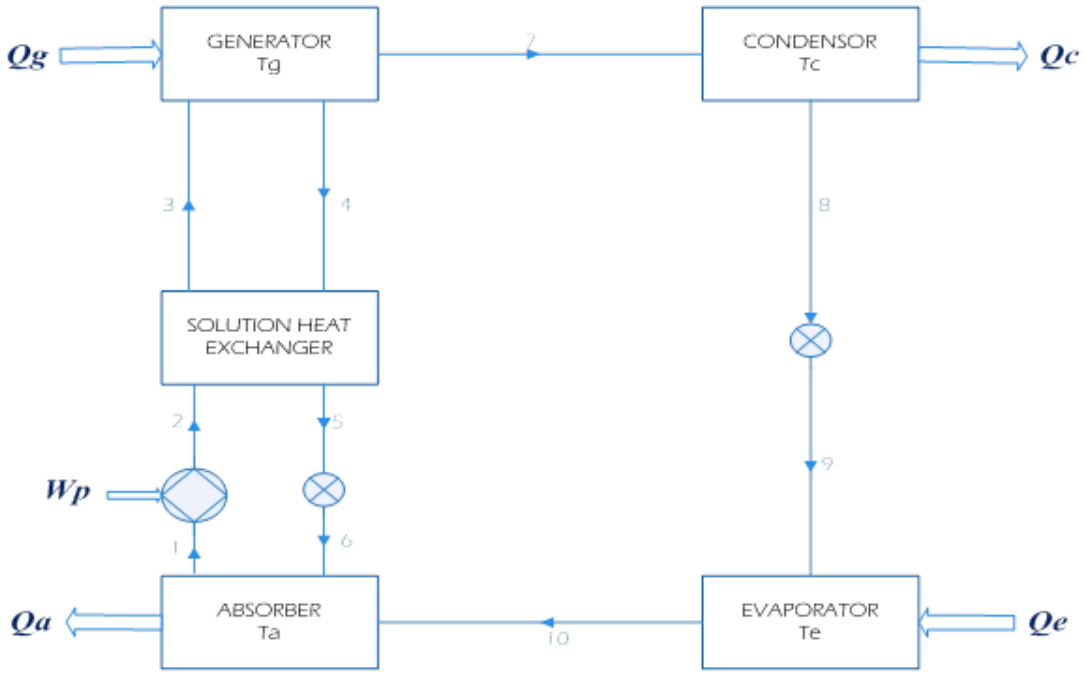

Figure 3: Schematic of A Single Effect LiBr-Water Absorption Cooling System.

In the absorber section, pressurization is accomplished via melting the refrigerant in the absorbent. It is important to evaporate the water at low-temperature in this cycle which is formed by injecting of chiller addicted to a profound vacuum.

The refrigerant vapor is drawn to absorber via concentration difference of amid LiBr solution. It is absorbed through absorption of LiBr solution combined with persistent boiling performance of refrigerant water. Along these lines the refrigerant vapor is compacted with more less mechanical energy demands than the vapor-compression air conditioning needs.

In the absorption chiller, as displayed in Figure 3.3, the refrigerant vapor is absorbed in liquid, stream1, while it rejected from the evaporator, stream 10. Consequently, the mixture is pressurized with a pump, stream 2, thus the refrigerant is heated and

separated from the mixture via the solution heat exchanger, stream 3. The expansion of heat in the generator is utilized to isolate the refrigerant from the solution. Consequently, corresponding to a common cooling system, the refrigerant goes to the condenser, stream 7, where the refrigerant vapour is cool down to form the water liquid. The refrigerant water flows into the evaporator, stream 8, through the refrigerant pump, stream 9, and pumps to the spray by the applying tool. Heat transfer from surrounding (cooling coil) to refrigerant instigated refrigerant water to turn to vapour, morever yielding chilled water. Ultimately, chilled water is forced to the cooling coil element for supplying cool air to the building. Then again, weak refrigerant fluid instantly flows back to the absorber from the generator section via the expansion valve, stream 4, and repeats the cycle.

3.1.3 Thermal Storage Tank

The accessibility of solar energy can not be configured the same, directly indicated by basic energy functions. It accumulates solar energy while the extent assembled is further than prerequisite of request thus release energy while total accumulation is deficient, therefore, the solar cycle drives stable.

The storage tank will probably work with a significant amount of thermal lamination and at the same time the liquid temperature will rise to the top of the storage tank. This circumstance primarily governed by the volume of the tank, the scale, position and target scheme of the intake and outputs in addition flow rates of inflowing as well as exiting flows.

3.2 System Mathematical Modelling

Capacity control is summarized in each section of the single-effect absorption cycle. Generator part, absorber, evaporator, condenser and heat exchanger, in addition, the

fan-coil and parabolic groove collector structure are used to evaluate the working conditions of all sections.. The mass and the energy stabilities are achieved indeed TRNSYS simulation is established pro the system investigation.

3.2.1 Single Effect Absorption Chiller

Absorption cooling system consists of a generator, a condenser, an evaporator and an absorber to be modelled by using mass and energy balance laws. The mass and energy balances for the chiller are as proposed by Kong, Liu, Zhang, He, and Fang [22]. schematic diagram of the proposed solar sourced single-stage ACS is indicated in Figure 4.

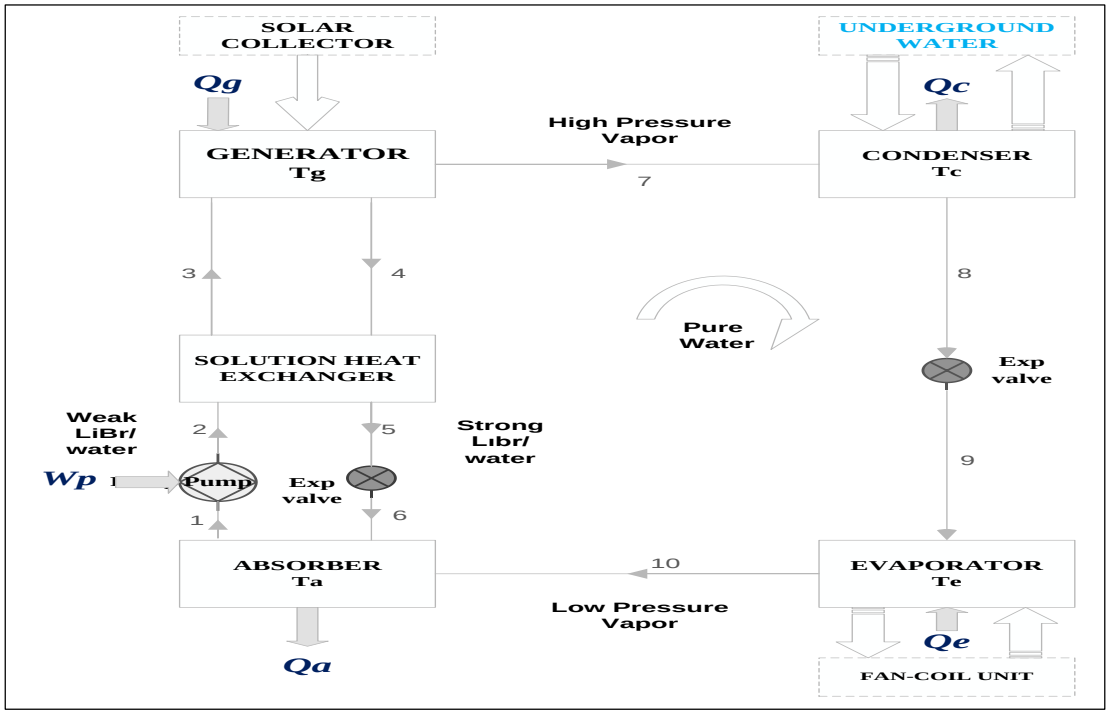

Figure 4: Schematic of the solar sourced single-stage absorption chiller structure.

Mass and energy equilibrium of each component of the proposed ACS cycle (Figure 4) were given in Equations 1-26 below;

$$x_1 = x_2 = x_3 = x_W \quad (1)$$

$$x_4 = x_5 = x_6 = x_s \quad (2)$$

where x_W defines weak mixture absorption and x_s defines strong mixture absorption. The mass balance equations through every single components of absorption cooling cycle are as follows:

$$\frac{dMg}{dt} = \dot{m}_3 - \dot{m}_4 - \dot{m}_7 \quad (3)$$

$$\frac{dMc}{dt} = \dot{m}_7 - \dot{m}_8 \quad (4)$$

$$\frac{dMe}{dt} = \dot{m}_9 - \dot{m}_{10} \quad (5)$$

$$\frac{dMa}{dt} = \dot{m}_{10} + \dot{m}_6 - \dot{m}_1 \quad (6)$$

$$\dot{m}_8 = \dot{m}_9 \quad (7)$$

$$\dot{m}_1 = \dot{m}_2 = \dot{m}_3 \quad (8)$$

$$\dot{m}_4 = \dot{m}_5 = \dot{m}_6 \quad (9)$$

where M states the mass of water, $\dot{m}$ is the water flow rate and superscripts 1 to 10 specifty input and output of per element, as presented in Figure 4.

The energy balances of the segments are contributed as:

$$\frac{d}{dt}(M_g h_g) = \dot{m}_3 h_3 - \dot{m}_4 h_4 - \dot{m}_7 h_7 + Q_g \quad (10)$$

$$\frac{d}{dt}(M_c h_c) = \dot{m}_7 h_7 - \dot{m}_8 h_8 - Q_c \quad (11)$$

$$\frac{d}{dt}(M_e h_e) = \dot{m}_9 h_9 - \dot{m}_{10} h_{10} + Q_e \quad (12)$$

$$\frac{d}{dt}(M_a h_a) = \dot{m}_{10} h_{10} + \dot{m}_6 h_6 - \dot{m}_1 h_1 - Q_a \quad (13)$$

$$W_p = \dot{m}_2 h_2 - \dot{m}_1 h_1 \quad (14)$$

$$h_8 = h_9 \quad (15)$$

$$h_5 = h_6 \quad (16)$$

where *h* indicates the enthalpy, *Q* sets as the amount of heat transfer, W_p sets as the pump work, and where superscripts *g*, *c*, *e*, *a* and *p* illustrates the generator, condenser,evaporator, absorber and pump.

The solar energy input to the generator is calculated with the Equation 17 below:

$$Q_g = \dot{m}_4 h_4 + \dot{m}_7 h_7 - \dot{m}_3 h_3 \quad (17)$$

The amount of heat rejected to the underground water in condenser is rendered via the following equation:

$$Q_c = \dot{m}_7 (h_7 - h_8) \quad (18)$$

The amount of heat absorption of the evaporator is presented as follow:

$$Q_e = \dot{m}_7 (h_{10} - h_9) \quad (19)$$

The amount of heat expulsion out of the absorber is given as follow:

$$Q_a = \dot{m}_{10} h_{10} + \dot{m}_6 h_6 - \dot{m}_1 h_1 \quad (20)$$

An energy balance of the hot side of the heat exchanger is written as follows:

$$Q_{HE-h} = \dot{m}_4 (h_4 - h_5) \quad (21)$$

Correspondingly energy balance for the cold side of the heat exchanger is presented in the following equation:

$$Q_{HE-c} = \dot{m}_3 (h_3 - h_2) \quad (22)$$

The total energy balance on the heat exchanger is fulfilled if $Q_{HE-h} = Q_{HE-c}$ that is valid in this case.

$$\varepsilon = \frac{h_4 - h_2}{h_4 - h_2} \quad (23)$$

where ε is defining the efficiency of heat exchanger and *h* indicates the enthalpy.

The temperature and enthalpy of LiBr-H_2 O mixture for any certain condition can be achieved via the following Equations:

$$T_{sol} = T_{ref} \sum_{i=0}^{3} a_i x^i + \sum_{i=0}^{3} b_i x^i \quad (24)$$

$$h_{sol} = \sum_{i=0}^{4} c_i x^i + T_{sol} \sum_{i=0}^{4} d_i x^i + {T_{sol}}^2 \sum_{i=0}^{4} e_i x^i \quad (25)$$

where the continuous factors of *a, b, c, d, e, i* were obtainable by Florides et al. (2003) and ASHRAE handbook (1997), T_{ref} is refrigerant temperature, T_{sol} is solution temperature and h_{sol} is enthalpy of solution [23].

An essential character to represents the property of the change of heat addicted to cold that called the COP, outlined as the valuable cold, Q_{cold}, each unit of contributed injected heat, Q_{hot}. COP corresponding to Figure 3.5 is expressed via following equation:

$$\text{COP} = \frac{Q_{Cold}}{Q_{Heat}} = \frac{Q_{eva}}{Q_{gen}} \quad (26)$$

Figure 5 [24]. indicates the COP diagram of sorption chillers via inlet hot water.

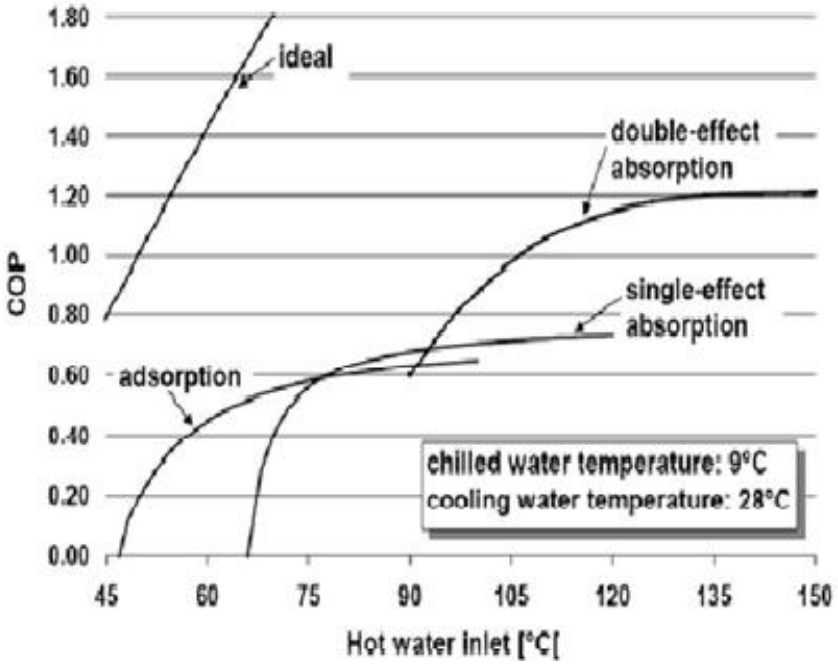

Figure 5: COP curves of sorption chillers [24].

According to ASHRAE, [23] amount of lithium bromide in solution must be less than 70% to avoid formation of salt crystals and more than 40% to absorb water in the absorber. The concentration of LiBr in strong solution is dependent on the absorber temperature and the evaporative temperature. Because the evaporation temperature is steady, the temperature of the absorber, which is equivalent to the ambient temperature, affects the strong solution concentration.

3.2.2 Parabolic Trough Solar Collector

Energy balance equations for parabolic trough collector modelled by Egbo et al, [25] measured the heat gain and the heat transfer between the sections, i.e. the mirroring surface, the glass shield and the absorber tube, the thermal properties of the materials and geometric dimensions of the solar parabolic trough collector.

The thermal efficiency of the parabolic trough collector is followed as;

$$\eta_{th} = 1 - \frac{Q_{losses}}{Q_{input}} \tag{27}$$

where Q_{losses} is the total heat losses of the collector and Q_{input} is the total heat contributed to the reciever.

The hourly heat supplied to the reciever (Q_{input}) can be figured as follow;

$$Q_{input} = \left[(I_{beam} * R_b) + I_{diff}\right] * [wL] \quad (28)$$

where I_{beam} is the beam radiation on a horizontal surface, R_b is the slope factor, I_{diff} is setting as the diffuse radiation, *w* is setting as the aperture width of the hub and *L* is setting as the length of concentrator.

The total heat losses in the system (Q_{loss}) is measured as the sum of the radiative, convective and conductive heat losses through the exterior part of the glass shield that be able to convey as follows;

$$Q_{loss} = q_{r_2} + q_c + q_1 \quad (29)$$

where q_{r_2} is the radiative heat loss through the surface of the glass cover to the exteriorities, q_c is the convectieve heat loss from the surface of the enveloping glass cover to the exteriorities and q_1 is the conductive heat loss from the fluid to the exteriorities.

3.2.3 Storage Tank

The storage tank can be displayed by multimode unidimensional type which partitioned the tank towards to “n” completely blended nodes [26]. Portion of “n” decides the level of lamination. Storage tank is displayed whereas a completely blended tank while n=1. Thus, multiple scope nodes be able to suppose. In this type, the flexible inlet sites are reflected, therefore the streams cross the nodes among adjacent density or temperature. This state conserves the greatest conceivable level of thermal lamination.

An energy stability on node I (I range from 1 to n) are recorded as:

$$m_i c_p \frac{dT_{s,i}}{dt} = \alpha_i \dot{m}_c c_p \left(T_c - T_{s,i}\right) + \beta_i \dot{m}_L c_p \left(T_L - T_{s,i}\right) + \delta_i \gamma_i c_p \left(T_{s,i-1} - T_{s,i}\right) + \quad (30)$$

$$(1 - \delta_i)\gamma_i c_p \left(T_{s,i} - T_{s,i+1}\right) - UA_{s,i}\left(T_{s,i} - T_a\right)$$

where

$$\alpha_i = \begin{cases} 1 & if\ i = 1\ and\ T_c > T_{s,i} \\ 1 & if\ T_{s,i-1} \geq T_c > T_{s,i} \\ 0 & otherwise \end{cases}$$

$$\beta_i = \begin{cases} 1 & if\ i = n\ and\ T_L < T_{s,n} \\ 1 & if\ T_{s,i} \geq T_L > T_{s,i+1} \\ 0 & otherwise \end{cases}$$

$$\delta_i = \begin{cases} 1 & if\ \gamma_i > 0 \\ 0 & if\ \gamma_i \leq 0 \end{cases}$$

m_i is the mass of the fluid of node I, c_p sets as the specific heat capacity of fluid, $T_{s,i}$ sets as the saturated temperature of node I, $\dot{m}_c$ sets as the collector fluid mass flow rate, T_c sets as the outlet fluid temperature of collector, $\dot{m}_L$ sets as the load mass flow rate, T_L sets as the fluid temperature coming from the load and $UA_{s,i}$ is the heat loss coefficient product of node I.

3.3 Economical Analysis

The payback period is the time extent entailed to recuperate the cost of an asset. The payback period of a presented project is a vital factor to hold the situation or project. longer payback periods are naturally not attractive for investment spots. The payback period discounts the time estimation of money, dissimilar to other techniques for capital planning, for instance net present value, internal rate of return or promotional cash flow. Life cycle cost (LCC) evaluating is a method for assessing the outline options financially via various asset, maintenance costs and setup costs. This technique is concerned while a venture requires high preliminary investment charges to

distinguish the economic viability. The amount of life cycle cost is equivalent the aggregate of the present estimations of the entire costs upon the life cycle of the projects involving savings and principal costs, erection and developement costs, conservation costs, energy costs, salvage costs, process costs and obliteration costs. All current and upcoming costs are improved to a solitary fact in the investment time via the present rate method [27].

The total cost of the solar system includes the capital cost of the solar panels, storage tank, additional cost of the absorption chiller over that of the conventional air-condition and the installation cost (assumed to be 10% of total capital cost of solar system).

Considering to evaluate the life cycle cost different factors be supposed to examined that are characterized in the subsequent.

- The lingering time estimated for life cycle cost is the evaluation period.
- The discount rate (R) is dictated by the distinctive financier centred on a complex assortment of factors. In a simple model, it can be considered as the annual interest rate of a credit used to fund a project which is taking into account 6% in this study.
- Residual value defines the upcoming value of the fraction of its preliminary value. Meanwhile, these factors are not decomposable following lifetime, zero is regarded for this issue.
- Saving to investment ratio (SIR) is consumed to figure out if the capacity of project accumulation supports the preliminary investment. Furthermore, SIR appointed as benefit-cost ratio, reconciles the present value of savings achieved

upon the investment's economic life to find the asset cost of the project at the present time. It covers the overall energy savings throughout the lifetime of the present value divided by the direct cost of the investment. It is stated as the formula:

$$\text{SIR} = \frac{\text{Present Value of Future Savings}}{\text{Initial Cost}} \tag{31}$$

If the SIR result achieves equal to 1.0, the present estimation of future funds is equivalent to the cash Money needed at the present time to accomplish those investment funds, in the event that the ratio gets below 1.0, therefore the Project will not create as much cash as a simple, safe investment would. on the off chance that the ratio surpasses 1.0, it displays the investment will issue a paying back which is better than the effectively acquired return [28].

- Internal rate of return (IRR) is measured and evaluated the visbility of assets. It is measured through expecting the net present value equivalent to zero.
- Simple payback period (SPP) is defined as the amount of time required for an investment to generate cash flows sufficient to recover its initial cost. Based on the payback rule, an investment is acceptable if its calculated payback period is less than some pre-specified number of years [29].

$$PBP = \frac{\text{initial investment}}{\text{cash flow per period}} = \frac{ln(C_{sys})}{ln(1+i)} \tag{32}$$

where C_{sys} is the cost of the system and i is the interest rate.

- The cost of the system is established via the following summation:

$$C_{sys} = C_{tank} + C_{collector} + C_{absorption\ chiller} + C_{pump} + C_{installation} \tag{33}$$

- Present Value (PV) is used to compute the current value of an amount that is received at the future [29].

$$PV = \frac{C_1}{(1+r)^n} \tag{34}$$

Where C_1 is the cash flow at period 1, r is the rate of return and n is the mark of periods.

- Ross, [29] defined net present value (NPV) as the summation of the present value of cash flows of a project. If the result of NPV is positive, a project should be accepted. In contract, if the NPV is in negative, the project should be rejected. If NPV is equal to zero, there is no difference in taking or rejecting the project. Summation of the present value of cash flows withdraws the net present value (NPV) of a project;

$$NPV = \sum_{i=0}^{n} \frac{C_1}{(1+r)^n} \tag{35}$$

Chapter 4

SIMULATION IN TRNSYS

4.1 TRNSYS

TRaNsient SYstem Simulation (TRNSYS) is a widely used, thermal process dynamic simulation program. It was originally developed for solar energy applications, and can now be used for a wider variety of thermal processes. TRNSYS was developed at the University of Wisconsin by the members of the solar energy laboratory and the first version was released in 1977 [30]. TRNSYS can be used for simulation of solar PV, solar heating and cooling and building energy. It has the capability to interconnect system components in any desired manner, solving differential equations and information output.

TRNSYS projects can be setup by use of the graphical interface in the 'Simulation Studio', or by manual coding of the model's response file (denoted to in place of the 'deck file'). The desired system is broken into individual components, each of which is referred to as a unit. Each unit in a system is characterized by a 'Type' (for example Type 4 is a stratified storage tank), and multiple instances of a Type can occur in a system. The Types are interconnected with one another to model the flow of energy, matter, or other variables. Each Type has a matching set of 'proformas' which describe the components' inputs, outputs, and parameters. Inputs are the time-dependent characteristics of the inlets to the Type (e.g., flow rate of inlet flow 1, temperature of inlet flow 1). Similarly, outputs describe the time-dependent characteristics of the

outlets of the Type (e.g., flow rate of outlet 1, temperature of outlet flow 1). According to the reaserches of the University of Wisconsin, [30] Parameters are the time-independent governing characteristics of the Type, e.g., the total component mass, and mass-weighted average specific heat for a pump. Each of the Types has an underlying mathematical model coded in FORTRAN or C++, which allows the user to program additional Types not currently available in the TRNSYS library [31].

The plant modelling in TRNSYS is accomplished through sequential explicit systems simulation, which involves successive substitution. At each time step, the outputs of the first unit are determined based on its parameters and inputs. The unit's outputs are then passed as the inputs to the succeeding units. The result of the successive substitutions is then used as the base for the following iteration to achieve convergence of the plant solution.

New models can be added without impacting the overall solution, allowing again for high levels of customization and model iteration. The limitation of the sequential method is seen in the instability of systems with little or no energy storage, and of systems which have multiple discrete states which rapidly change [32]. The system created in TRNSYS is pronounced in beyond detail in the subsequent parts. Figure 6 provides the schematic of the system model developed in TRNSYS within the Simulation Studio.

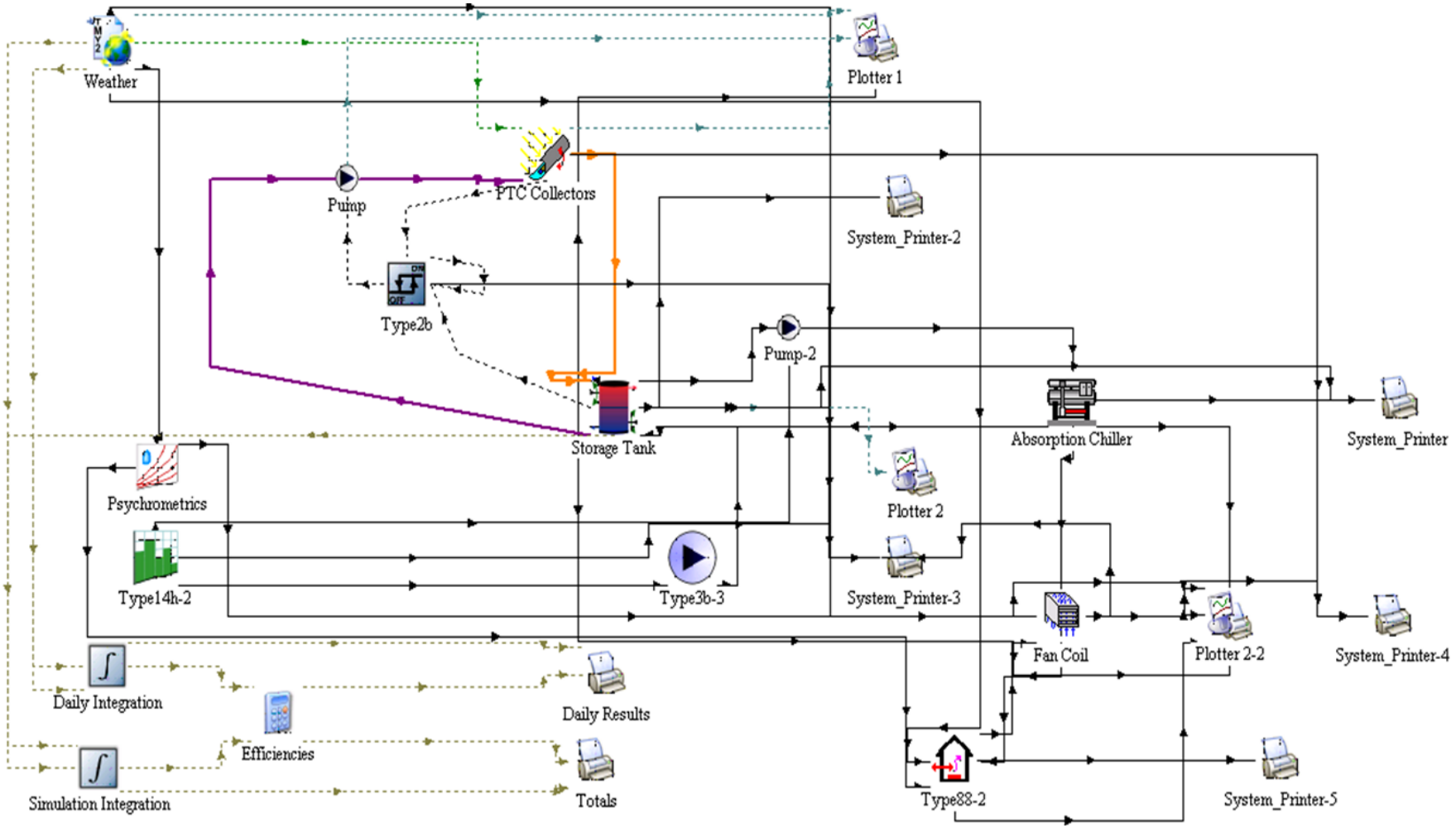

Figure 1: Layout of the PTC solar absorption cooling model settled in TRNSYS within the Simulation Studio

4.2 TRNSYS Components and System Models

In order to accurately model this system, existing TRNSYS Types were used for the components. TRNSYS software comprises of several subprogrammes that model sub-system apparatuses. The types which been used to model the cooling system are the followings:

i. Weather data (Type 109)

ii. Hot water buffer storage (Type 4a)

iii. Single-effect Absorption Chiller (Hot water fired Type 107), the main model component. Its Mathematical equations and internal calculation steps are described in detailed in section (4.2.3).

iv. The sort of the solar collector is significant as well as corresponding to the process and efficiency of the entire structure. In this research, Parabolic Trough collectors are considered and modelled with TRNSYS Type 73.

v. Some of circulating pumps are (Type 3). Type 3 is a model for "single speed pump" (constant flow rate). Its ON and OFF function driven by control signals of differential controller.

4.2.1 Type 109 - Weather Data (TMY2)

The classification was demonstrated with the TRNSYS software program. TRNSYS contains a variety of weather data with different weather data types. The main types available are TMY, TMY2 and TMY3 (for US), EPW, CWEC, IWEC and Meteonorm for all the major cities of the world.

The recreation design is established to occur per hour run of radiation and temperature data via Larnaca, Cyprus, which is the neighbouring city of Famagusta . The hourly averages time series of universal horizontal radiation along with temperature have

been used a Typical Meteorological Year version 2 (TMY2), which are available in the weather library of the TRNSYS simulation environment. The particularized monthly dry bulb temperature and monthly average humidity ratio of Larnaca during summer season (mid-June to mid-September) is shown in Figure 7.

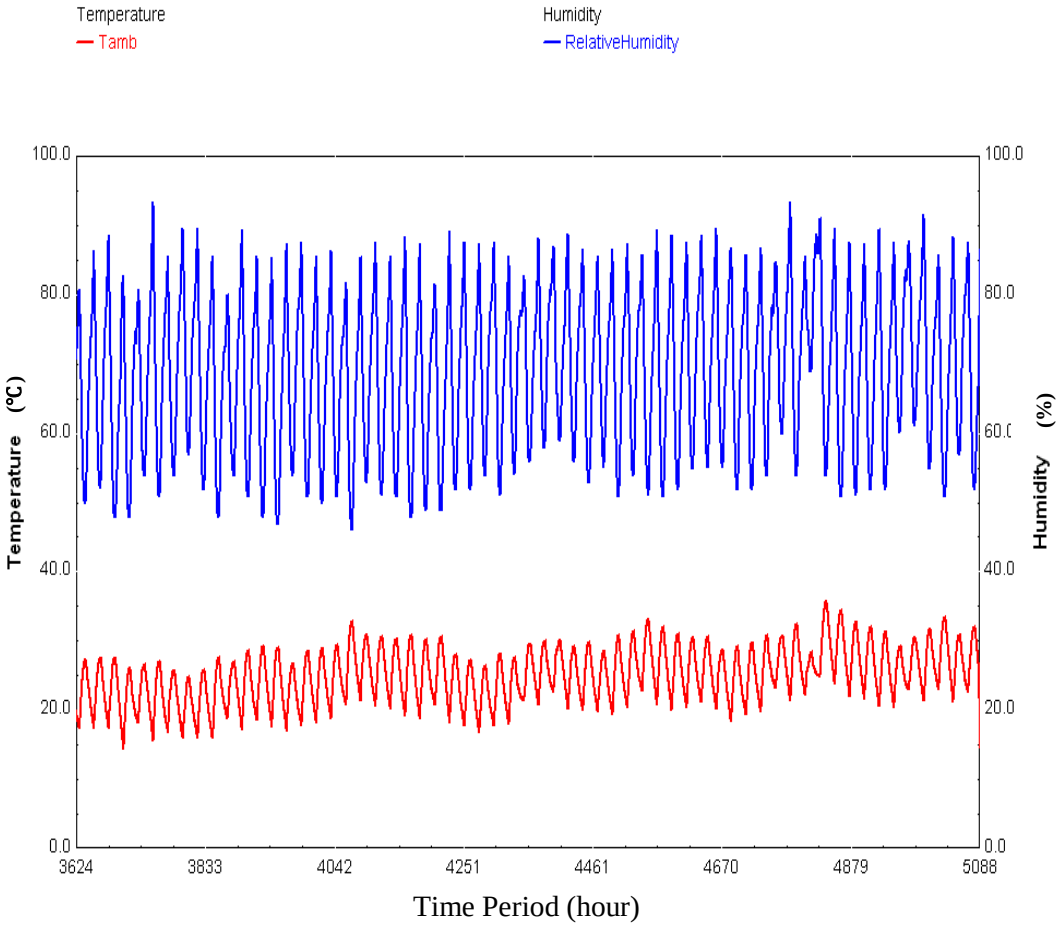

Figure 7: The ambient temperature and relative humidity results of Larnaca extended by TRNSYS programming.

Figure 8 virtually describes the total radiation of solar irradiance simulated in TRNSYS software the use of Larnaca weather conditions.

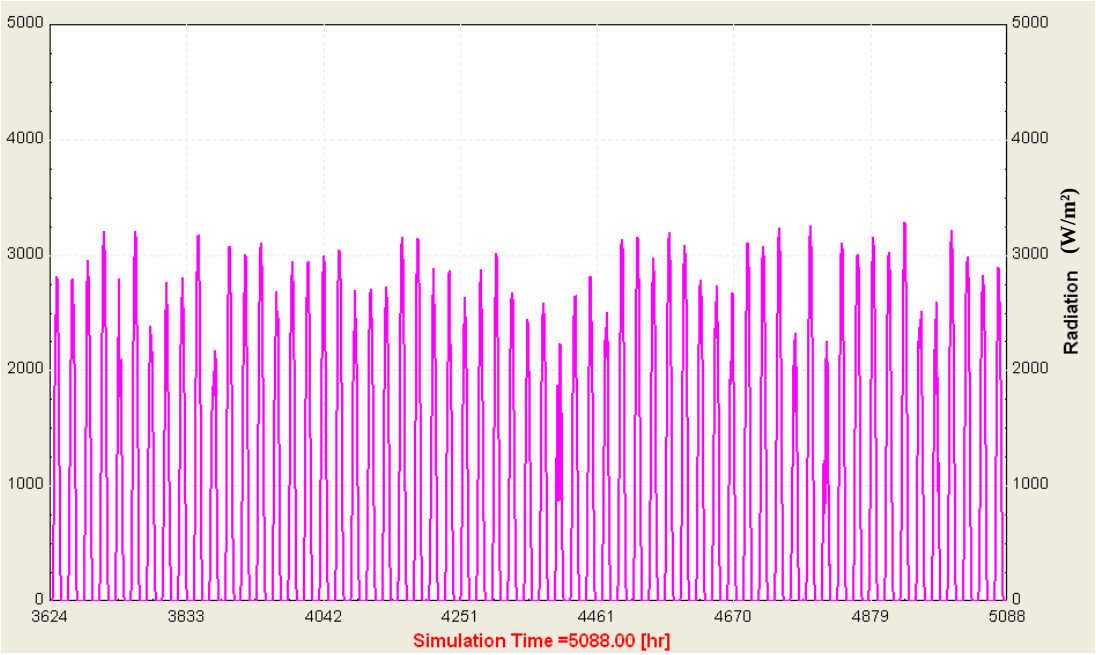

Figure 8: Hourly total radiation of Larnaca weather conditions at summer season achieved by TRNSYS program.

4.2.2 Type 4a – Storage Tank

Type 4 is consumed to purpose the storage tank. To object a storage tank works by stable inputs and constant losses Type 4a is able to use. This type of storage tank contains an auxilary heater to control the minimum outlet temperature of water (settled 80 ˚C in this project) flowing through the ACS. With the purpose of avoiding the tank water to boil, the higher bound of the outlet tank water temperature was arranged as 98℃. This type of storage tank was modelled with 15 nodes. These nodes afforded a sensible simulation run time, as well as have been produced accurate temperature divisions via TRNSYS design studies [33]. It is a stratified storage tank with fixed inlets and uniform losses with an auxiliary heating system. The stratified tank delivers water at a slightly higher temperature than an unstratified tank. This is a simple stratified tank suitable only as a storage tank without auxiliary heating. The tank volume is 3 m^3 with a total height of 1m and an area of 3 m^2 and a diameter of 1.6m. This volume is sufficient to provide energy for 24 hour operation of an absorption chiller with about 12 hour back up. Tank Type4a includes two auxiliary heating

elements and auxiliary heating elements are not used in this simulation so their maximum heating capacity is set to zero [34]. To pretend existent settings several controllers (Type 2b) are engaged. The controllers are supervise the collector stream be influenced by the contrast of the liquid temperature beyond the collector line.

Fluid is hot on the top side and cools down as it moves downwards and is cold at the bottom of the tank. The tank is divided into ten equal heights (each 0.10m). It was assumed that losses from each tank node are equal. The hot water from the collector enters the tank top and leaves from the top to the chiller. The cold side water enters at the bottom of the tank returning from the chiller and leaves the tank bottom for the inlet to the collector as shown in Figure 6-26, where, mh and mL are the fluid flow rates to and from the heating side and load side respectively and the temperature difference from top to bottom is about 10°C [34].

4.2.3 Type 107 – absorption chiller

The custom absorption chiller Type 107 is a simple component which performs an energy balance on the given input flows based on a control strategy. For the initial dimensioning of the system, a constant COP was selected for simplicity as an appropriate baseline for the sizing of the system. For this study, a constant COP of 0.7 was selected based on previous experiments such as Grossman [35].

Figure 9, displays the COP obtained in multiple experiments completed with the use of LiBr-water absorption chiller with a chilled water set point of 7˚C [36]. From this figure, it can be seen that a COP of 0.7 is an appropriate conservative value for the initial sizing of the single-effect system.

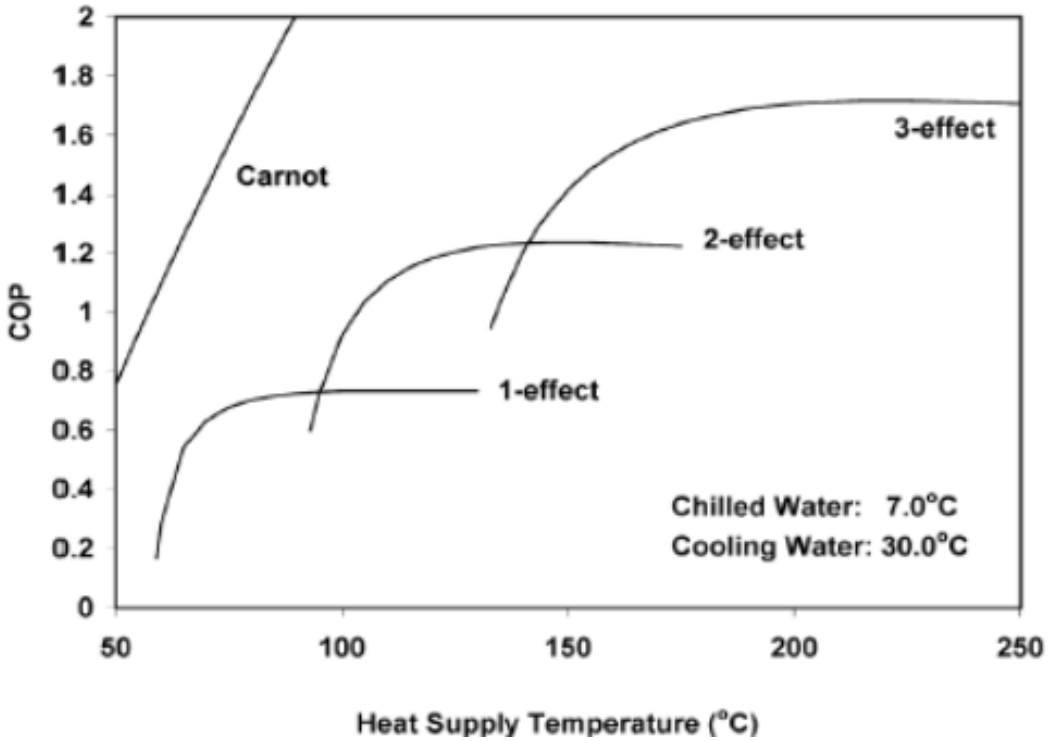

Figure 9: COP for instance the task of solar heat source temperature for LiBr-water absorption chiller [35].

The Japanese company Yazaki (Yazaki Aroace WFC-SC10) is sufficient to protect the cooling power, room temperature of the 35 kW junk cooling power at a set point of 25 ° C instead of 100% of all working hours. Table 1 gives the technical data of Yazaki Aroace WFC-SC10 Chiller [36].

Table 1: The technical data of the Yazaki Aroace WFC-SC10 Absorption Chiller [36].

STANDARD SPECIFICATIONS

	Specifications		WFC-	SC10	SH10	SC20	SH20	SC30	SH30	SC50
	Cooling Capacity		MBTUh (kW)	120.0 (35.2)		240.0 (70.3)		360.0 (105.5)		600.0 (175.8)
	Heating Capacity		MBTUh (kW)	---	166.3 (48.7)	---	332.6 (97.5)	---	498.9 (146.2)	---
Chilled/Hot Water	Temperature	Cooling	°F (°C)	54.5 (12.5) Inlet / 44.6 (7.0) Outlet						
		Heating	°F (°C)	117.3 (47.4) Inlet / 131.0 (55.0) Outlet / (WFC-SH Models Only)						
	Evaporator Pressure Loss		PSI (kPa)	8.1 (55.8)		9.6 (66.2)		10.1 (69.6)		6.4 (44.2)
	Max Operating Pressure		PSI (kPa)	85.3 (588.1) / (High Pressure Option Available on WFC-SC50 only)						
	Rated Water Flow		GPM (l/s)	24.2 (1.5)		48.4 (3.1)		72.6 (4.6)		121.1 (7.6)
	Allowable Water Flow Range		% of Rated	80% - 120%						
	Water Retention Volume		Gal (liters)	4.5 (17.0)		12.4 (46.9)		19.3 (73.1)		33.6 (127.2)
Cooling Water	Heat Rejection		MBTUh (kW)	291.4 (85.4)		582.8 (170.8)		874.2 (256.2)		1457.0 (427.0)
	Temperature	Cooling	°F (°C)	87.8 (31.0) Inlet / 95.0 (35.0) Outlet						
	Absorber Pressure Loss		PSI (kPa)	12.3 (84.8)		6.6 (45.5)		6.7 (46.2)		6.6 (45.3)
	Condenser Pressure Loss		PSI (kPa)	Included in Absorber		6.6 (45.5)		6.7 (46.2)		3.2 (21.9)
	Max Operating Pressure		PSI (kPa)	85.3 (588.1) / (High Pressure Option Available on WFC-SC50 only)						
	Rated Water Flow[1]		GPM (l/s)	80.8 (5.1)		161.7 (10.2)		242.5 (15.3)		404.5 (25.5)
	Allowable Water Flow Range		% of Rated	100% - 120%						
	Water Retention Volume		Gal (liters)	17.4 (65.9)		33.0 (124.9)		51.3 (194.2)		87.2 (330.1)
Heat Medium	Heat Input		MBTUh (kW)	171.4 (50.2)		342.8 (100.5)		514.2 (150.7)		857.0 (251.2)
	Temperature		°F (°C)	190.4 (88.0) Inlet / 181.4 (83.0) Outlet						
	Allowable Temperature Range		°F (°C)	158.0 - 203.0 (70.0 - 95.0)						
	Generator Pressure Loss		PSI (kPa)	13.1 (90.3)		6.7 (46.2)		8.8 (60.7)		13.6 (93.7)
	Max Operating Pressure		PSI (kPa)	85.3 (588.1) / (No High Pressure Option)						
	Rated Water Flow		GPM (l/s)	38.0 (2.4)		76.1 (4.8)		114.1 (7.2)		190.4 (12.0)
	Allowable Water Flow Range		% of Rated	30% - 120%						
	Water Retention Volume		Gal (liters)	5.5 (20.8)		14.3 (54.1)		22.2 (84.0)		39.7 (150.3)
Electrical	Power Supply			208 volts AC / 60 Hz / 3-Phase						
	Consumption[2]		Watts	210		260		310		670
	MCA		Amps	0.6		0.9		2.6		4.7
	MOCP		Amps	15						
Construction	Dimensions[3]	Width	Inches (mm)	29.9 (760)		41.7 (1060)		54.3 (1380)		70.3 (1785)
		Depth	Inches (mm)	38.2 (970)		51.2 (1300)		60.8 (1545)		77.2 (1960)
		Height	Inches (mm)	74.8 (1900)		79.1 (2010)		80.5 (2045)		82.1 (2085)
	Weight	Dry	lbs (kg)	1100 (500)		2050 (930)		3200 (1450)		4740 (2150)
		Operating	lbs (kg)	1329 (603)		2548 (1155)		3975 (1800)		5955 (2700)
	Noise Level		dB(A)	49				46		51
Piping	Chilled/Hot Water		Inches	1-1/2 NPT		2 NPT				3 NPT
	Cooling Water		Inches	2 NPT				2-1/2 NPT		3 NPT
	Heat Medium		Inches	1-1/2 NPT		2 NPT		2-1/2 NPT		3 NPT

Note: All metric values are calculated from the Imperial values and are only approximate values.

1 - Minimum cooling water flow is 100%.
2 - Power consumption does not include external pumps or motors.
3 - Width/Depth does not include the junction box or mounting plates. Height does not include the removable lifting lugs but does include level bolts.

A logical variable was output from the Type 107 for each time step that indicated whether the chiller has actuated at that time step or not. When not actuating, the flow rate and temperature of each of the water streams flowing into the chiller remained unchanged. This strategy was equivalent to implementing a control on the pump which would only allow the water streams to flow to the chiller when actuated. When the

chiller was actuated, a simple energy balance was used to determine the outlet temperature of each of the streams. The first calculation performed by Type 107 was to determine the required heat rejection energy to reduce the chilled water stream to the chilled set point. Equation 36 describes this relationship:

$$\dot{Q}_{chill} = \left(T_{chill,in} - T_{setpoint}\right) \times \dot{m}_{chill} \times C_{chill} \quad (36)$$

where $\dot{Q}_{chill}$ is the energy removed from the chilled water stream in *W*, $T_{chill,in}$ is the temperature of the chilled water inlet in ℃, $T_{setpoint}$ is the setpoint temperature of the chilled water outlet in ℃, $\dot{m}_{chill}$ is the flow rate of he chilled water in *kg/s*, and C_{chill} is the heat capacity of the chilled fluid in *kJ/kg ℃*(in this case water).

Type 107 then checked to ensure that *Q* was below the rated capacity of the chiller (53kW). If the required energy was above the rated capacity, then Q was set to 53 kW, and then outlet temperature of the chilled stream (T_{chill}) was calculated using Equation (35);

$$T_{chill,out} = T_{chill,in} - \left(\frac{\dot{Q}_{chill}}{\dot{m}_{chill} \times C_{chill}}\right) \quad (37)$$

If the required energy was below the rated capacity, the calculated value of $\dot{Q}_{chill}$ was retained and the outlet temperature of the chilled stream gets started the chiller setpoint. The energy removed from the chilled water stream was then used to calculate the required energy from the heated stream ($\dot{Q}_{hot}$), as described by Equation 38;

$$\dot{Q}_{hot} = \frac{\dot{Q}_{chill}}{COP_{in}} \quad (38)$$

The COP and auxiliary power (P_{Aux}) were both parameters input by the user. As stated before, the COP was considered to remain constant at 0.7, and the auxiliary power provided by the Yazaki guidelines, [37] was 210 W. The outlet temperature of the hot stream was then calculated using Equation (37), replacing all the chilled water values with those of the hot water stream.

The heat transferred to the heat rejection stream ($\dot{Q}_{heat,rejection}$) was calculated using Equation (39). The outlet flow rates of each of the streams were equated to the incoming flow rates.

$$\dot{Q}_{heat,rejection} = \dot{Q}_{hot} + \dot{Q}_{chill} + P_{Aux} \quad (39)$$

Equation (36) through (39) provides the mathematical model for the absorption chiller Type, which was then used in conjunction with other system components and controls.

4.2.4 Type 536 - Linear Parabolic Concentrator Solar Collector

This subroutine models a linear parabolic Trough collector, which addicted to a solar collector essence solar radiation. Category of the structure is based on the absorbed parabolic concentrate (orifice) that mirrors the sun irradiance against a cylinder-shaped absorber tube.

Direct absorbers be able to converge beam radiation to the absorber tube while the sun is at the dominant level surface of the absorber. The surface sheet comprising the central alignment along with the apex streak of the reverberator. Type 536 is able to spin around a solitary shaft of swirl, that possibly will be North to South or East to West otherwise oblique along with analogous to the axle of the earth, that in this situation the amount of spin is fifteen degrees per hour. The substantial variances are

subsisted in cooperation amount of incident beam radiation, it belongs to the time, in addition the picture property achieved by the 3 styles of process. This model neglects the diffuse radiation and uses the linear collector efficiency equation to model the concentrator.

The solar inputs for this collector should be output from the TYPE 16 radiation processor operating in modes 2 or 3 for tracked surfaces. This subroutine requires an external data file which contains the incidence angle modifiers as a function of incidence angle (up to 10˚). Refer to the information on the Logical unit parameter for more information on this data file. The solar collector will defocus part of the array conserving the outlet temperature less than an addict- stated maximum; calculating the "dumped" energy if an over-temperature condition would occur.

4.2.5 Type 3 – Pump

Type 3 figures out the mass flow rate which utilizing a flexible control function (contains a value among 1-0) along with a stable extreme flow volume. In this type, pump power is able to be estimated the both, as a direct function of mass flow rate along with through an operator distinct connection among mass flow rate as well as power ingesting. The user determinate part of the power of the pump is adapted to liquid thermal energy. This element locates the flow rate instead of the other segments in the stream loop by multiplying the maximum flow rate with the control signal.

Chapter 5

RESULTS AND DISCUSSION

5.1 Energy and Coefficient of Performance Analysis

The case study considered in this work on solar absorption refrigeration system presents a sustainable method to meet the air conditioning demand in buildings in Famagusta. The size and properties of the Absorption chiller (Yazaki Aroace WFC-SC10) has been adapted to comply with the cooling demand of building.

The performance of the system is concerned by several issues. These issues are the storage tank volume, the collector area, the generator input temperature, the condenser inlet temperature and the building zoon. Numerous simulation outputs were achieved in turns of the consideration of these issues' consequences on the system operation, but only the factor of "inlet cooling water temperature" is investigated statistically. The numerous simulations were devoted to verify the COP along with the drawbacks of the ACS performing orders. Attributable to estimate the ACS performing process, compared with variant formerly given alignments, founded results are displayed via using TRNSYS software program. Initial variable settings, which are assumed via the use of equations previously given in Chapter 4, are shown in Table 2;

Table 2: Initial variable conditions for SACS [38].

Variable	**Initial conditions**	**Range varied** [38]
Solar collector flow rate	0.21 *kg/s*	0.05 *kg/s* – 0.25 *kg/s*
Solar collector area	30 m^2	10 m^2 to 35 m^2
Solar storage tank volume	3 m^3	0.6 $m^3 - 3\ m^3$
Fluid specific heat	4.19 *kJ/kg.k*	
Cooling load capacity (Yazaki WFC-SC10)	35 *kW*	15 kW – 53 *kW*
Hot water inlet Temperature (T_g)	98 ℃	70 ℃ - 105℃
Hot loop flow rate	1.365 *kg/s*	0.035 *kg/s* per *kW*
Cooling water inlet Temperature (T_C , T_a)	22℃	19 ℃ - 34℃
Cooled loop flow rate	2.275 *kg/s*	0.05 to 0.11 *kg/s* per *kW*
Chilling water inlet temperature (T_e)	12.2℃	6 ℃ - 17℃
Chilled loop flow rate	1.505 *kg/s*	0.03 to 0.05 *kg/s* per *kW*

The COP actually depends on the evaporation temperature, the basis for forming the preferred cold load, the temperature of the generator as well as the outlet temperature and the condenser of the cooler. Figures 10-11 analysis demonstrates the COP variation in the proposed single effect ACS for the different condenser and constant generator and the evaporator temperatures for a hot day in Famagusta (August 15th) with peak solar radiation of 937 W/m^2.

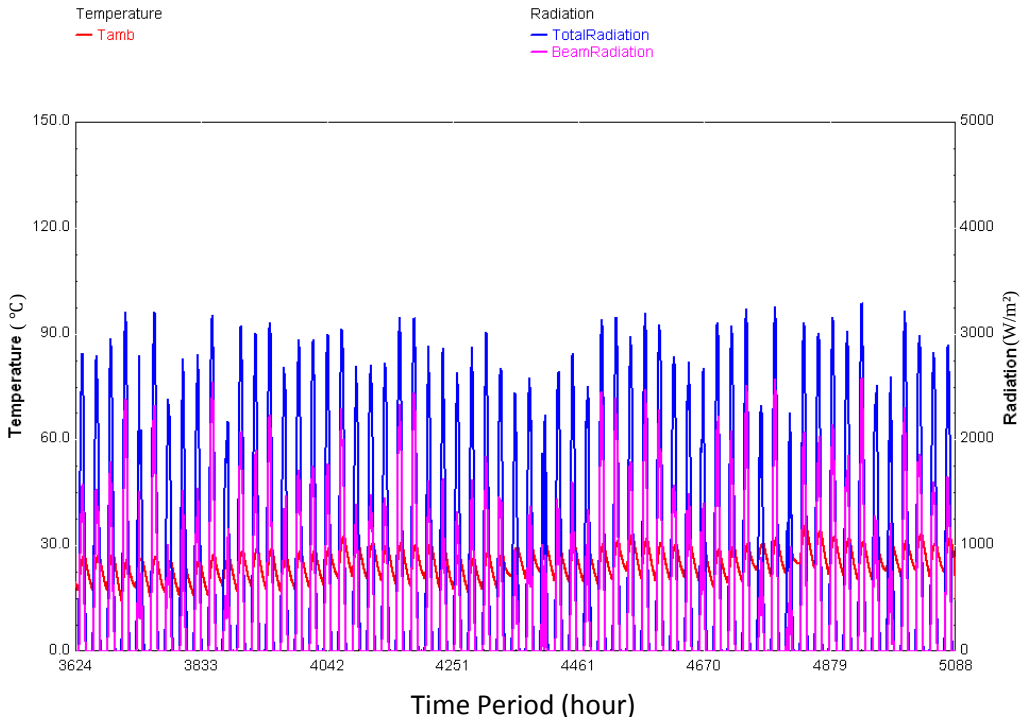

Figure 10: Ambient temperature versus Radiation in Famagusta among summer season (June15th – September15th)

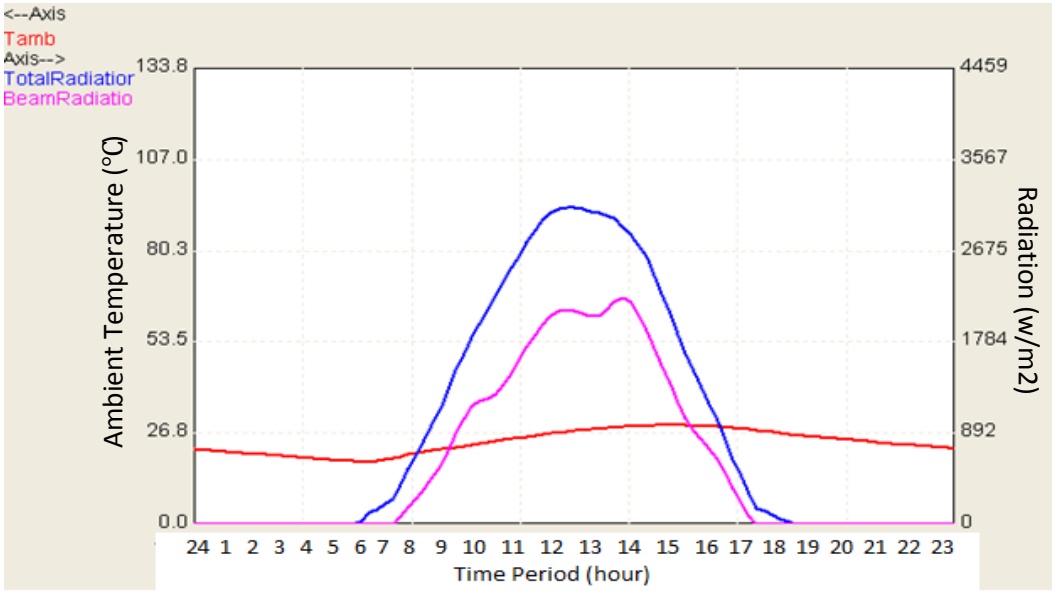

Figure 11: Ambient temperature versus total Radiation and beam radiation at 15th of August.

As seen in Figure 11, the peak ambient temperature is 34℃ and the average solar radiation is approximately 3350 w/m^2 on 15th of August in Larnaca the nearest city to Famagusta. The results of COP differences in the various inlet condenser temperatures

in the range of 15-32℃ are yielded by TRNSYS as shown in the Figure 5.3 at a hot summer day (August 15th). The results displayed that the max COP is 0.672 at the inlet temperature of 15℃ and the minimum COP of the system is equal to approximately 0.5051 at the inlet condenser temperature of 32℃.

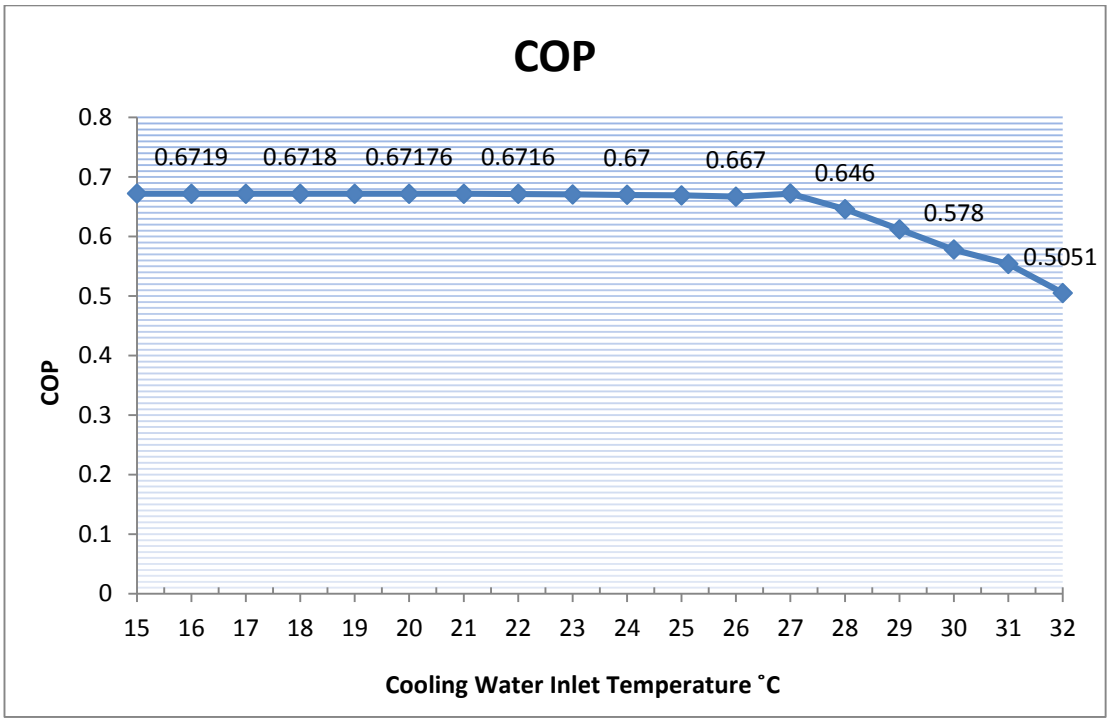

Figure 12: COP differences of ACS versus the various inlet condenser temperatures at 15th of August in Famagusta.

According to Figure 12, the COP of a single effect ACS rises up among the condenser temperature decreasing, that the COP of the system is greater for low value of T_C instead of the fixed T_e and T_g.

The output energy comparison of the three components of a desired single stage ACS, Evaporator (Q_e), Condenser (Q_c) and Generator (Q_e) are simulated through adjusting the several temperatures ranges as the inlet cooling temperature to the condenser from 32℃ regularly to 15℃, the results achieved by TRNSYS program are shown in

following Figures in Famagusta. (see Figure 13, Figure 14, Figure 15). The simulation is performed hourly whole the summer season (June 15th-September 15th).

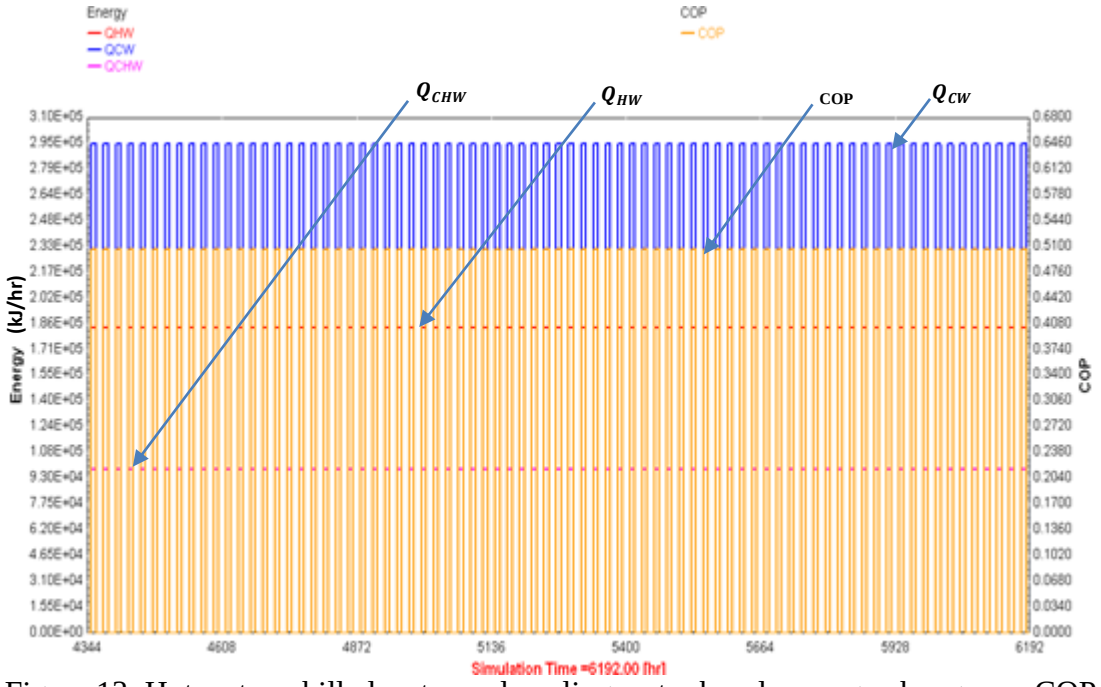

Figure 13: Hot water, chilled water and cooling water hourly energy changes vs COP during summer season (mid-June to mid-September) in Famagusta at (T_Cooling=32℃)

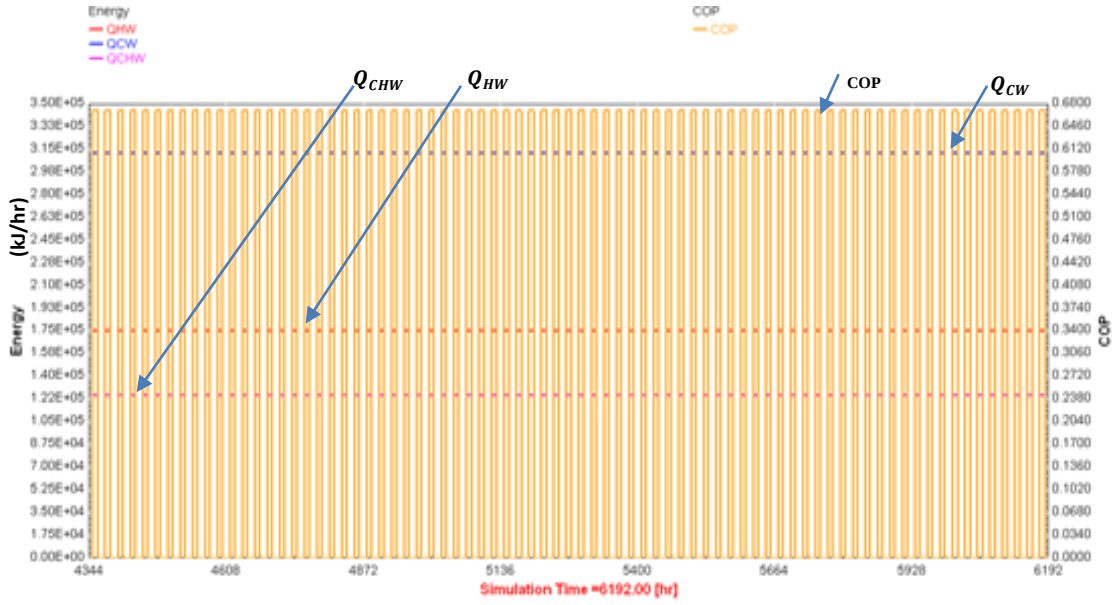

Figure 14: Hot water, chilled water and cooling water hourly energy changes vs COP during summer season (mid-June to mid-September) in Famagusta at (T_Cooling=22℃)

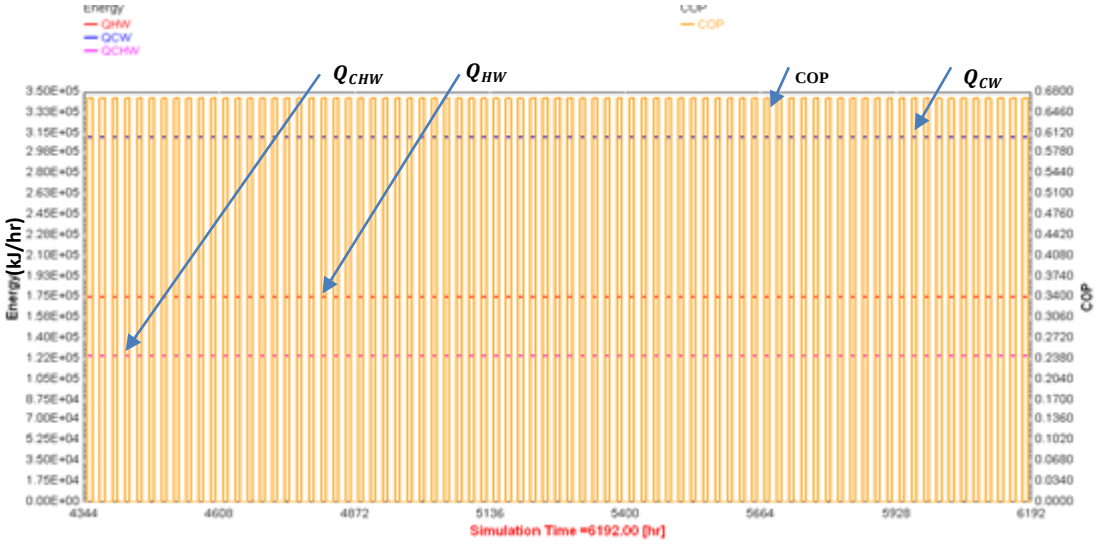

Figure 15: Hot water, chilled water and cooling water hourly energy changes vs COP during summer season (mid-June to mid-September) in Famagusta at (T_Cooling=15℃)

Throughout every simulation run operations, each variable of all components were assumed as steady state except the cooling water temperature at the condenser stream. Several simulations were formly progressed, respectively via a distinct value for the inlet cooling *Tc*. The identical method was subsequently reiterated instead of each variable. The assortment beyond which per variable was altered is displayed in Figure 16.

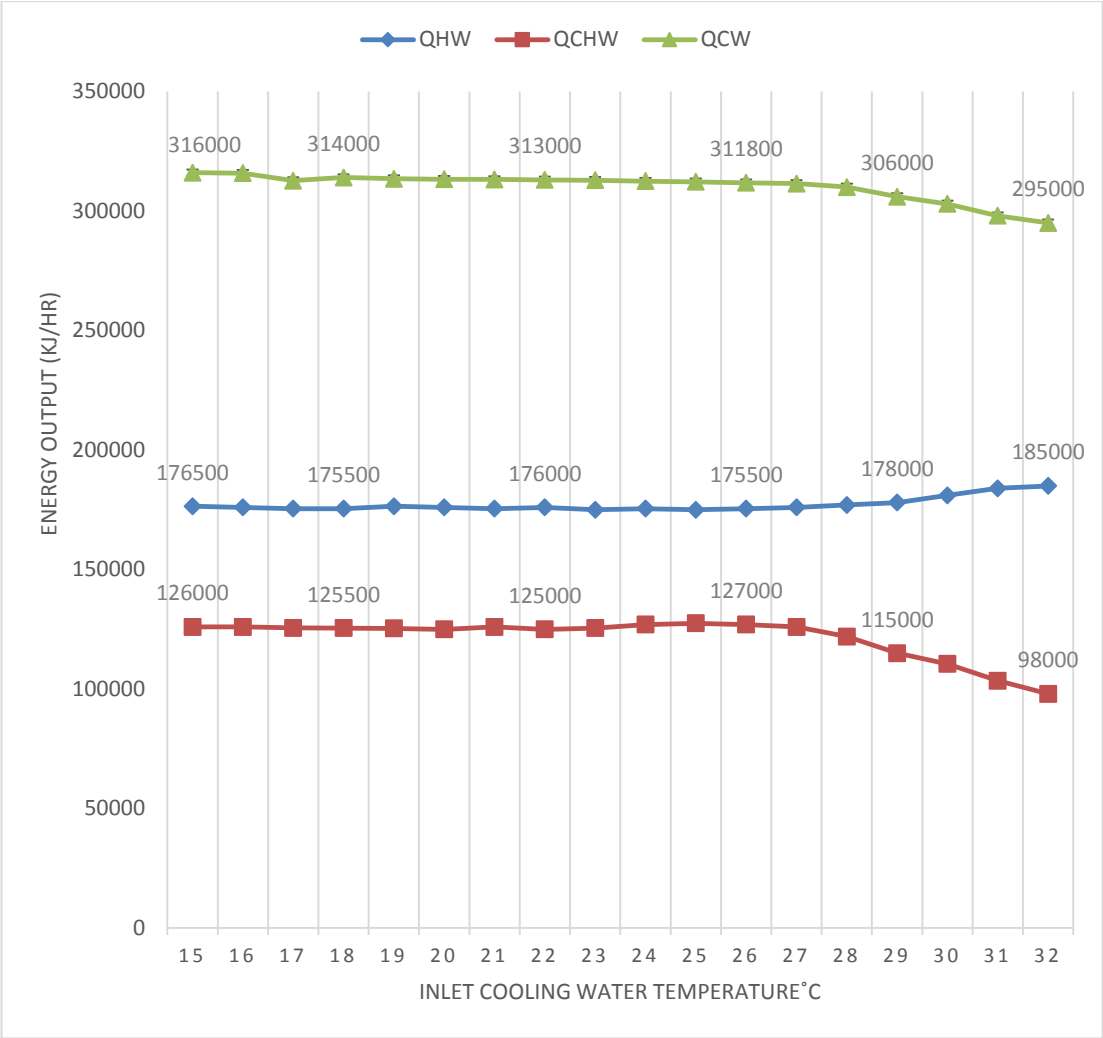

Figure 16: Comparison of the energy outputs of the ACS components versus the different condenser inlet temperature at 15th of August.

The outcomes from TRNSYS program, which are detected hourly in hot summer day (15th of August) are distinctly represented in Table 3. The results apportioned for the specification of the system to every single components.

Table 3: Comparison of different inlet cooling water temperatures in Famagusta (August 15th).

Inlet Tc (˚C)	**COP**	Q_{HW}	Q_{CHW}	Q_{CW}
15	0,672	176500	126000	316000
16	0,6719	176000	126000	315800
17	0,6718	175500	125600	312700
18	0,6718	175500	125500	314000
19	0,67178	176500	125400	313500
20	0,67176	176000	125000	313300
21	0,67168	175500	126000	313200
22	0,6716	176000	125000	313000
23	0,6708	175000	125500	312900
24	0,67	175500	127000	312500
25	0,669	175000	127500	312200
26	0,667	175500	127000	311800
27	0,672	176000	126000	311500
28	0,646	177000	122000	310000
29	0,612	178000	115000	306000
30	0,578	181000	110500	303000
31	0,554	184000	103500	298000
32	0,5051	185000	98000	295000

According to Figure 16, the maximum energy of the generator (heating water), the condenser (cooling water) and the evaporator (chilling water) are respectively founded as 176500 *kJ/hr*, 316500 *kJ/hr* and 126000 *kJ/hr*, which are detected among with 15℃

inlet cooling water temperature. Furthermore, the minimum energy outputs of the generator, the condenser and the evaporator are correspondingly obtained as 185000 *kJ/hr*, 295000 *kJ/hr* and 98000 *kJ/hr* at the identic period (August 15th) in Famagusta.

The resolution of the energy in competition with COP's assessments among variant cooling temperatures indications that the coefficient of performance rises up as the condensation temperature reduces as well as the energy outputs of the condenser and the evaporator increase. Besides, as described in section 1.4, the average underground water temperature in Famagusta is approximately 22℃ the whole summer season period, however the cooling tower is commonly used for absorber and condenser components in ACSs, which the water temperature obtained by the cooling tower is about 33-30 ℃. Then through using the underground water in Famagusta for condenser water cooling, we can increase the COP of the system as well as the energy output of the evaporator, which is utilized to obtain the chilling water using in cooling loads (fan coil in this project). Figure 17 and 18 show that the COP and energy output of three basic ACS components, evaporator, condenser and generator is maximum for the underground water used condenser in place of cooling tower operated condenser.

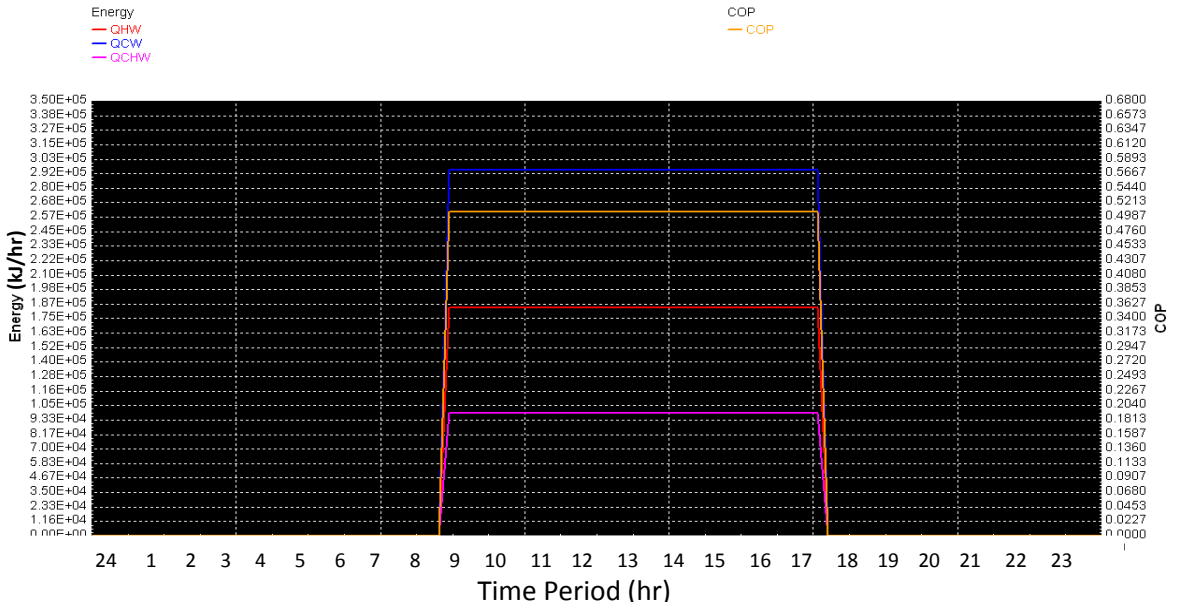

Figure 17: Hot water, chilled water and cooling water hourly energy changes vs COP during summer in Famagusta at (T_Cooling = 32℃).

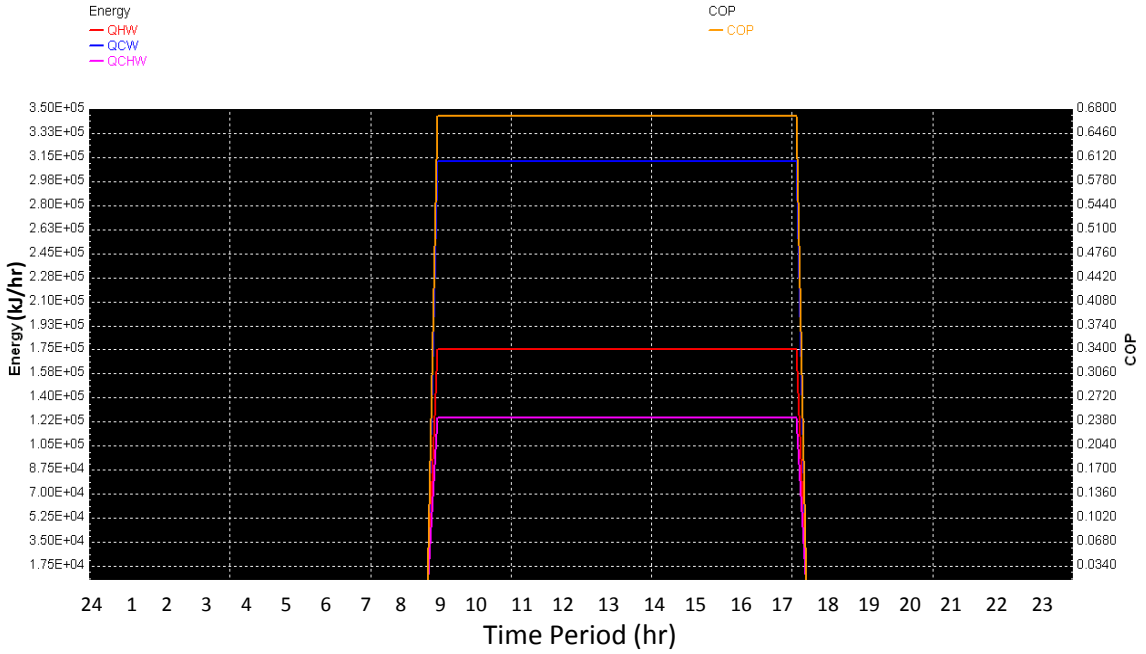

Figure 18: Hot water, chilled water and cooling water hourly energy changes vs COP during summer in Famagusta at (T_Cooling = 22℃).

The previous Figures show that the cooling water temperature averages don't hold the great affect upon the spread of the energy outputs of ACS however on the other hand, it has the major influence on the coefficient of performance of the system. The most

important gain of the operating the underground water instead of the cooling tower is that it can decrease the cost of investment as well as the saving costs, operating and maintenance costs during the system managing.

The absorption power of LiBr solution is stronger at lower temperature of the cooling water. When the temperature of the cooling water in the condenser is low, condensing temperature of the refrigerant decreases. Therefore, condenser pressure becomes low. As the boiling temperature (generator temperature) of the Li Br solution decreases when the condensing pressure is low, calorific value of the driving heat source can decrease. This will result in energy savings.

It is not acceptable that the temperature of cooling water is too low. The lithium bromide solution of certain concentration becomes crystallized under the temperature lower than certain degree. For example, at a concentration of LiBr of 65% this absorbent solution crystallizes at a temperature lower than 42°C, with concentration of 60% at a temperature lower than 17°C and with concentration of 55% at the temperature lower than 15°C. As the absorbent crystallizes, it become a solid, thus unable to flow therefore chiller cannot operate. In addition, it leaves a messy maintenance work of cleaning the whole system [39]. Thus, to avoid the crystallization of LiBr solution in absorber and condenser, the cooling temperature in absorption chiller is fixed to 22°C. By this reason, the COP and energy output results are taken constant at the condenser temperatures below 22°C.

5.2 Economic Analysis Results

In favour of estimating the economic analysis of the assumed SACS for a 200m^2 office building in Famagusta, firstly a building characteristics should be presented. The office

building with no solar apparatus is computed in the role of a source case. The source building is used the compressor air conditioner as a cooling load, which the electricity is consumed as the cooling power to cool the area. However, the electrical power cost is 0.2 $/kWh in Cyprus.

Therefore, it desired to use the SACS as a remedy of decreasing the electricity costs to the assumed office building sourced case, that the system involves a parabolic trough solar collector along with hot buffer tank and an 35kW single stage absorption chiller. The total price of the SACS contains the investment cost of parabolic trough panel, hot water storage tank, the hot water driven absorption chiller as the common air conditioner along with the installation cost, which is expected to be 10% of the whole investment cost. The simulation and components cost results of solar sourced single stage absorption chiller is individually shown in Table 4.

Table 4: Simulation results of single effect SACS [40].

Parabolic trough solar collectors (6)	Reflector aperture area (m^2)	30
	Field cost ($/$m^2$)	270
	Estimated cost ($) [41]	24,300
Hot water storage tank	Tank volume (m^3)	3,0
	Estimated cost ($)	1,163
Absorption chiller	Cooling capacity (kW)	35
	COP	0.672
	Estimated cost ($)	54,000
Total investment cost	Estimated cost ($)	**79,463**

Working days of the office building in hot season (June-September) is 92 days and the working hours are 9 hours per day. Therefore, yearly energy saving is obtained according to the defined assessments, that is worth 28,980 kWh and the anual saving in energy bill estimated as 5,796$ for the supposed office building. Financial analysis are estimated in proportion to the equations defined in section 3.4, the results are shown in Table 5.

Table 5: Life cycle investment scheme.

Year	New	Old	Net Amount
0	$80.809		$80.809
1			$0
2			$0
3		$250	-$250
4	$520		$520
5			$0
6		$250	-$250
7			$0
8	$520		$520
9		$250	-$250
10		$1.250	-$1.250
11			$0
12	$520		$520
13		$250	-$250
14			$0
15			$0
16	$520	$250	$270
17			$0
18			$0
19		$250	-$250

Annual Savings	$5.796
Discount Rate	10%
Analysis period (years)	25
Residual value	$8.080

Table 6: Results of NPV, SIR and IRR values.

Net Present Value (NPV)	**-$31 256**
Savings-to-Investment Ratio	**0,6**
Internal Rate of Return (IRR)	**4%**
Simple Payback (years)	**13,9**

Economic analysis of this study presented yearly energy savings of 5,796$ for the SACS installed office building regarding to 4,636$ annual savings throughout the common 28 kW vapor compression system, among the SPP of 13,9 years. According to the obtained results, supposed project is not sufficient among the negative worth of the NPV and long period of SPP. This type of SAC is not financially feasible for the small residential places because of the great investment costs of solar panels and absorption chillers.

SIR chart shown in Figure 19 compares the relative merits of competing project implementation alternatives and assists the decision maker to accept or reject a project and prioritise accepted projects.

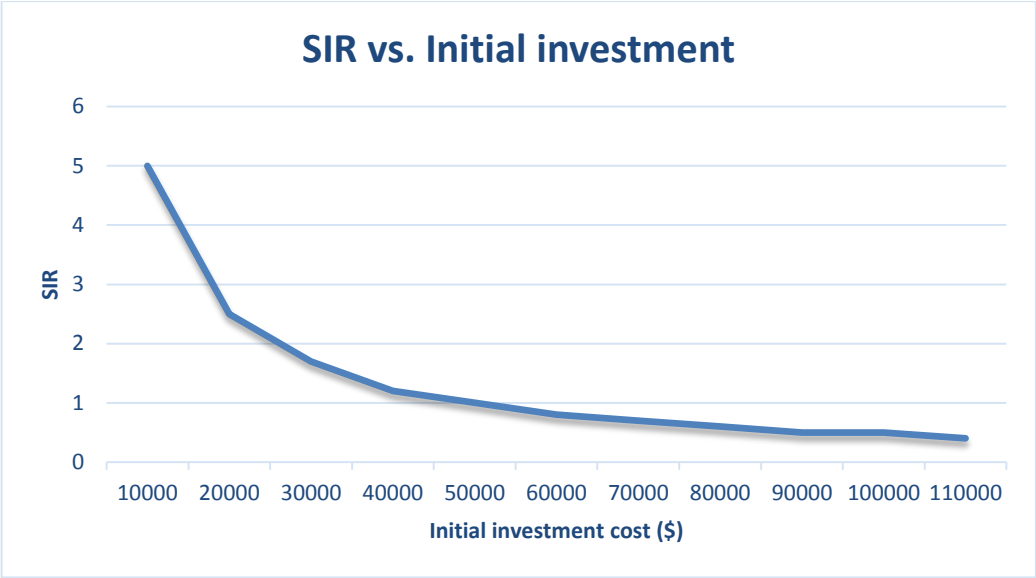

Figure 19: Saving to Investment Ratio versus the initial investment.

Therefore, considering to the chart of SIR vs initial investment cost, if the initial investment cost were to fall below 45000$ the project would be feasible at this point. The IRR and SPP rates versus the initial investment costs are shown in Figure 20 and 21.

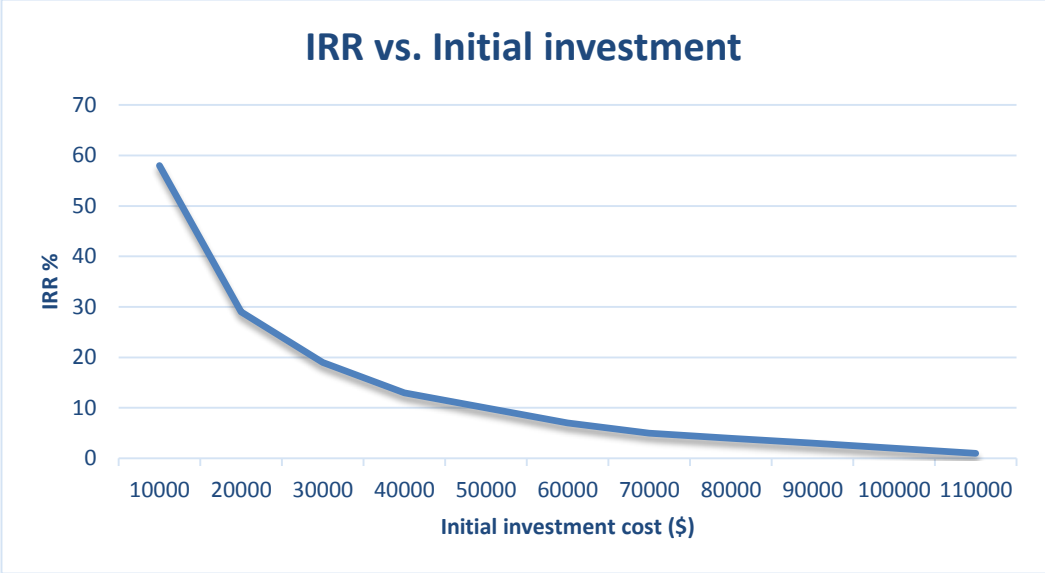

Figure 20: Internal rate of return versus the initial investment cost.

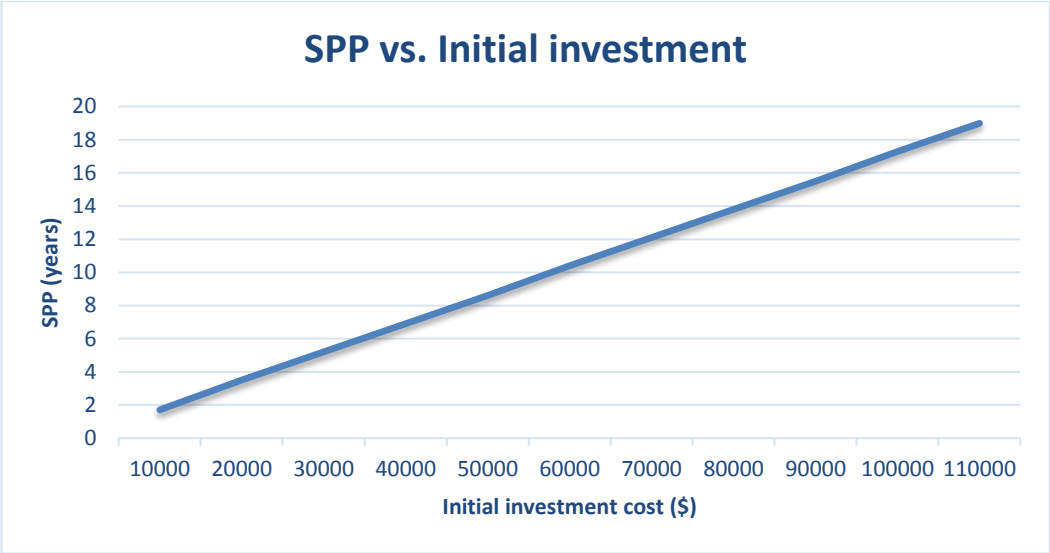

Figure 21: Simple payback period versus the initial investment cost.

Through the earned results as figured in previous charts, to make the project feasible, the investment cost of the simulated solar driven absorption chiller should be worth below 50,000$.

Chapter 6

CONCLUSION

Transient modelling of a solar driven absorption chiller proficiency was assessed grounded on the hourly weather data exploiting TRNSYS software program. Thus, it converts distinct that the authorised TRNSYS pretend model, in concurrence through Larnaca weather data, be able to apply in the function of a valuable engineering design apparatus to forecast the long-term running of a SCS lacking essentially functioning costly sample or full scale testing. The consequences attained as of the parametric optimization of the pretended SACS specify that the 30 m^2 parabolic trough collectors among 35˚ incline and 3,0 m^3 of storage tank and the LiBr-water single effect absorption chiller 35 kW cooling capacity (Yazaki WFC-SC10) can assure the cooling demand of a 200 m^2 office building positioned in Famagusta, Cyprus. Upcoming developments of this work will comprise the development of an overall cost model to be settled in the office building for investigational analyses and model proof over actual climatic conditions.

The COP and energy outputs of evaporator, generator and the condenser for different cooling water temperatures analysis were also displayed by TRNSYS program, determining the optimum values of the condenser inlet cooling temperature. The results gained, represented the lower inlet cooling temperature of the condenser effected the higher COP and energy outputs of ACS components. The underground water in Famagusta is approximately 22℃, therefore, it is able to operate it in the

function of 32℃cooling tower that is used as the cooling water in condenser. The COP is obtained 0.672 due to exploit the underground water in Famagusta. Thus, it is recommended that the underground water is supplementary desirable contrast with the cooling tower water to apply in the condenser.

A computer simulation is carried out for base case of a conventional system consisting of an electric powered air-conditioner. It was found that the operating energy cost of the office building comes to $4,636 electricity cost used for space cooling. Based on the results obtained from TRNSYS software program for a parabolic trough solar collector single effect LiBr-water absorption chiller, the following conclusions can be made:

1. The payback period, which obtained 13,9 years for this project, tends to decrease along with the decreasing the initial investment costs and increasing the COP of the system.
2. The net present value obtained is -$31,256 along with the SIR and IRR values estimated as 0.6 and 4%, thus the supposed project is not feasible in this case.

It is proposed that, the initial investment cost below $50000 can make the supposed project feasible.

REFERENCES

[1] Cyprus Meteorological Department. (2014). Department of Meteorology. Retrieved January 01, 2017, from the World Wide Web: http://www.moa.gov.cy/moa/ms/ms.nsf/Dmlcyclimate_en/DMLcyclimate_en.html

[2] American Gas Cooling Center, (AGCC), (1996). *Natural Gas Cooling Equipment Guide,* 4th Edition.

[3] World Weather and Climate Information. (2016). Average Monthly Rainfall-Temperature-Sunshine,Famagusta,Cyprus. Retrieved February 08, 2017, from the World Wide Web: https://weather-and-climate.com/average-monthly-Rainfall-Temperature-Sunshine,Famagusta,Cyprus.html

[4] Isik, B., & Tulbentci, T. (2008, September). Sustainable housing in island conditions using Alker-gypsum-stabilized earth: A case study from northern Cyprus. *Building and Environment, 43*(9), 1426 - 1432.

[5] Mokhtar MA., M., Brauniger, S., Afshari, A., Sgouridis, S., Armstrong, P., & Chiesa, M. (2010). Systematic comprehensive techno-economic assessment of solar cooling technologies using location: specific climate data. *Applied energy,* 87, 3766-78. ISSN 0306-2619.

[6] Dinçer, Đ., & Rosen, M.A. (2005). Thermodynamic aspects of renewables and sustainable development. *Renewable and Sustainable Energy Reviews*, 9, 169-189.

[7] Otanicar, R., & Phelan, P. (2012). Prospects for solar cooling: An Economic and Environmental Assessment. *Solar Energy*, 86, 1287-99. ISSN 0038-092X.

[8] Wang, S.K. (2001). *Handbook of air conditioning and refrigeration*: Chapter 14 Refrigeration systems: Absorption. Mc Graw-Hill.

[9] Utlu, Z., & Hepbasli, A. (2007). A review and assessment of the energy utilization efficiency in the Turkish industrial sector using energy and exergy analysis method. *Renewable and Sustainable Energy Reviews*, 11, 1438-1459.

[10] Florides, G.A., Kalogirou, S.A., Tassou, S.A., & Wrobel, L.C. (2003). Design and construction of a LiBr-water absorption machine. *Energy Conversion and Management*, 44, 2483-2508.

[11] N.K. Ghaddar, M., & Shihab, F., (1997). Modeling and simulation of solar absorption system performance in Beirut. In *Renewable energy* (Vol. 10(4), pp. 539-558).

[12] R. Lizarte, M., Izquierdo, J. D., & Marcos, E. (2012). An innovative solar-driven directly air-cooled LiBr/H2O absorption chiller prototype for residential use. In *Energy Build* (Vol. 47, pp. 1-11).

[13] D. Chemisana, J., Lopez-Villada, A., & Coronas, R. J. (2012). Building integration of concentrating systems for solar cooling applications. In *Applied Thermal Engineering* (pp 1-8).

[14] F. Assilzadeh, S. A., Kalogirou, Y., & Ali, K. (2005). Simulation and optimization of a LiBr solar absorption cooling system with evacuated tube collectors. In *Renewable Energy* (Vol. 30, pp. 1143-1159).

[15] Blinn, J. C., Mitchel, J. W., & Duffie, J. A. (1979). Modeling of transient performance of residential solar air-conditioning system. *In: Proceeding of the ISES Silver Jubilee Congress* (Vol. 1, pp. 705-709). Atlanta: Georgia.

[16] Charters, W. WS., & Chen, W. D. (1979). Some design aspects of air cooled solar powered LiBr-H2O absorption cycle airconditioning systems. In *Proceedings of the ISES,* Silver Jubilee Congress (Vol. 1. pp.725-8) Atlanta: Georgia.

[17] Ferrer, P. (2008). Enhanced efficiency of a parabolic solar trough system through use of a secondary radiation concentrator, *South African Journal of Science* (Vol. 104, pp. 9-10).

[18] Yong, K., Gui, Y. H., & Taebeom, S. (2008). *An evaluation on thermal performance of CPC solar collector,* International Communications in Heat and Mass Transfer 35, 446–457.

[19] Duffie, J. A., & Beckman, W. A. (1991). *Solar Engineering of Thermal Processes,* New York, 2nd Ed., John Willey & Sons.

[20] Johnson, G. (2011). Design and Commissioning of an Experiment to Characterize the Performance of a Lithium-Bromide Absorption Chiller. Ottawa: Carleton University.

[21] United Nations Environment Program (2006). Refrigeration & Air Conditioning System, *Vapor Compression Refrigeration System*. United Nations Environment Program (UNEP).

[22] Kong, D., Liu, J., Zhang, L., He, H. & Fang, Z. (2010). Thermodynamic and experimental analysis of an ammonia-water absorption chiller. *Energy and Power Engineering*, 2(04), pp. 298.

[23] ASHRAE. (1972). Absorption air-conditioning and refrigeration equipment. In: *ASHRAE Guide and Data Book*, Equipment. Chapter 14. New York.

[24] Henning, H. M. (2005). Solar Assisted Air Conditioning of Buildings – An Overview, *Heat Transfer in Components and Systems for Sustainable Energy Technologies*, France, 5-7.

[25] Egbo, G. I., Sambo A. S. & Asere, A. A. (1993). Development of Energy Equations for Parabolic-trough Solar Collector. *Nigerian Journal of Engineering Research and Developement*. 4(1), pp. 28-36.

[26] Kleinbach, E. M., Beckman W. A., & Klein S. A. (1993). Performance study of one-dimensional models for stratified thermal storage tanks. *Solar Energy* 50(2), 155-166.

[27] Atikol, U., Dagbasi, M., & Guven, H. (1999). Identification of residential end-use loads for demand-side planning in northern Cyprus. *Energy, 24*(3), 231 - 238.

[28] Dilouie, C. (Eds.). (2005). Advanced lighting controls: energy Savings, Productivity, *Technology and Applications.* USA.

[29] Ross, S. A. (2010). Fundamentals of Corporate Finance. McGraw Hill. Solar Server: Online Portal to Solar Energy. (n.d.). Retrieved Feb 09, 2017, from the World Wide Web: http://www.solarserver.com/knowledge/lexicon/k/kwp.html

[30] University of Wisconsin. (2010). TRNSYS 17 Documentation. Madison: Solar Energy Lab.

[31] Vidal, H., Escobar, R., & Colle, S. (2009). Simulation and Optimization of a Solar Driven Air Conditioning.

[32] Keiholz, W., Kummert, M., & Riederer, P. (2003). CSTB. Retrieved June 10, 2017, from Type 155 - a new TRNSYS type for coupling TRNSYS and MATLAB: Example of using 177 Matlab controllers with TRNSYS components: http://kheops.champs.cstb.fr/simbadlab/workshop/Presentation4.html

[33] Cruickshank, C. A., & Harrison, S. (2006). Simulation and Testing of Stratified Multi-Tank, *Thermal Storages for Solar Heating Systems*. Eurosun. Glasgow.

[34] Duffie, J. A., & William A. B. (2006). Solar Engineering of Thermal Processes, Fourth Edition, USA: John Wiley & Sons. 928.

[35] Grossman, G. (2002). Solar-Powered Systems for Cooling, Dehumidification and air-conditioning. *Solar Energy*, 53-62.

[36] Aroace. (2010). Water Fired Single-Effect Absorption Chiller and Chiller-Heater. Plano Texas: Yazaki Energy Systems, Inc.

[37] IEA (2014). Heating without Global Warming. Market Developments and Policy considerations for Renewable Heat. Retrieved Oct 20, 2016 from the World Wide Web: http://www.iea.org/publications/freepublications/publication/FeaturedInsightHeatingWithoutGlobalWarming_FINAL.html.

[38] AHRI Standard 566-2000, 2000 Standard for Absorption Water Chilling and Water Heating Packages, 2000, Air-Conditioning, Heating and Refrigeration Institute, 2111 Wilson Boulevard, Suite 500, Arlington, VA 22201, U.S.A.

[39] Bhatia, B. E. (2012). Overview of Vapor Absorption Chilling Systems. Retrieved February 10, 2017 from the World Wide Web: http://www.pdhonline.com/courses/m130/m130content.html

[40] Yilmazoglu, M. Z., & Amirabedin. E. (2012). The Verification of the Payback Time for a Solar Driven Absorption Cooling System Depending on Technological Development and Design Data. *Gazi University Journal of Science,* 25(3), 793-780.

[41] CSP Today. (2015). CSP Today Global Tracker. Retrieved September 02, 2016 from the World Wide Web: http://social.csptoday.com/tracker/projects.html

APPENDICES

Appendix A: Numerous Valued Capacities of YAZAKI's Chillers

Table 7: A.1: Different Capacities of YAZAKI's Chillers

Specifications			WFC-	SC5	SC/SH10	SC/SH20	SC/SH30	SC50
Cooling Capacity			Mbtuh	60.0	120.0	240.0	360.0	600.0
Heating Capacity (WFC-SH Only)			Mbtuh	---	166.3	332.6	498.9	---
Chilled/Hot Water	Cooling Temperature		°F	54.5 Inlet / 44.6 Outlet				
	Heating Temperature		°F	117.3 Inlet / 131.0 Outlet (WFC-SH Models Only)				
	Evaporator Pressure Loss		PSI	7.6	8.1	9.6	10.1	6.4
	Max Operating Pressure		PSI	85.3 / (High Pressure Option on WFC-SC50 only)				
	Rated Water Flow		GPM	12.1	24.2	48.4	72.6	121.1
	Allowable Water Flow		% of Rated	80% - 120%				
	Water Retention Volume		Gal	2.1	4.5	12.4	19.3	33.6
Cooling Water	Heat Rejection		Mbtuh	145.7	291.4	582.8	874.2	1457.0
	Temperature		°F	87.8 Inlet / 95.0 Outlet				
	Absorber Pressure Loss		PSI	5.6	12.3	6.6	6.7	6.6
	Condenser Pressure Loss		PSI	5.6	Included in Absorber	6.6	6.7	3.2
	Max Operating Pressure		PSI	85.3 / (High Pressure Option on WFC-SC50 only)				
	Rated Water Flow[2]		GPM	40.4	80.8	161.7	242.5	404.5
	Allowable Water Flow		% of Rated	100% - 120%				
	Water Retention Volume		Gal	9.8	17.4	33.0	51.3	87.2
Heat Medium	Heat Input		Mbtuh	85.7	171.4	342.8	514.2	857.0
	Temperature		°F	190.4 Inlet / 181.4 Outlet				
	Allowable Temperature		°F	158.0 - 203.0				
	Generator Pressure Loss		PSI	11.2	13.1	6.7	8.8	13.6
	Max Operating Pressure		PSI	85.3 / (No High Pressure Option)				
	Rated Water Flow		GPM	19.0	38.0	76.1	114.1	190.4
	Allowable Water Flow		% of Rated	30% - 120%				
	Water Retention Volume		Gal	2.6	5.5	14.3	22.2	39.7
Electrical	Power Supply			115 / 60 / 1	208 volts AC / 60 Hz / 3-Phase			
	Consumption[2]		Watts	48	210	260	310	670
	Minimum Circuit Amps		Amps	0.89	0.6	0.9	2.6	4.7
	MOCP		Amps	15				
Capacity Control				On - Off				
Construction	Dimensions[3]	Width	Inches	23.4	29.9	41.7	54.3	70.3
		Depth	Inches	29.3	38.2	51.2	60.8	77.2
		Height	Inches	69.1	74.8	79.1	80.5	82.1
	Weight	Dry	lbs	805	1100	2050	3200	4740
		Operating	lbs	926	1329	2548	3975	5955
	Noise Level		dB(A)	38	49		46	51
Piping	Chilled/Hot Water		Inches	1-1/4 NPT	1-1/2 NPT	2 NPT		3 NPT
	Cooling Water		Inches	1-1/2 NPT	2 NPT		2-1/2 NPT	3 NPT
	Heat Medium		Inches	1-1/2 NPT		2 NPT	2-1/2 NPT	3 NPT

Appendix B: Operation Data of YAZAKI Absorption Chillers

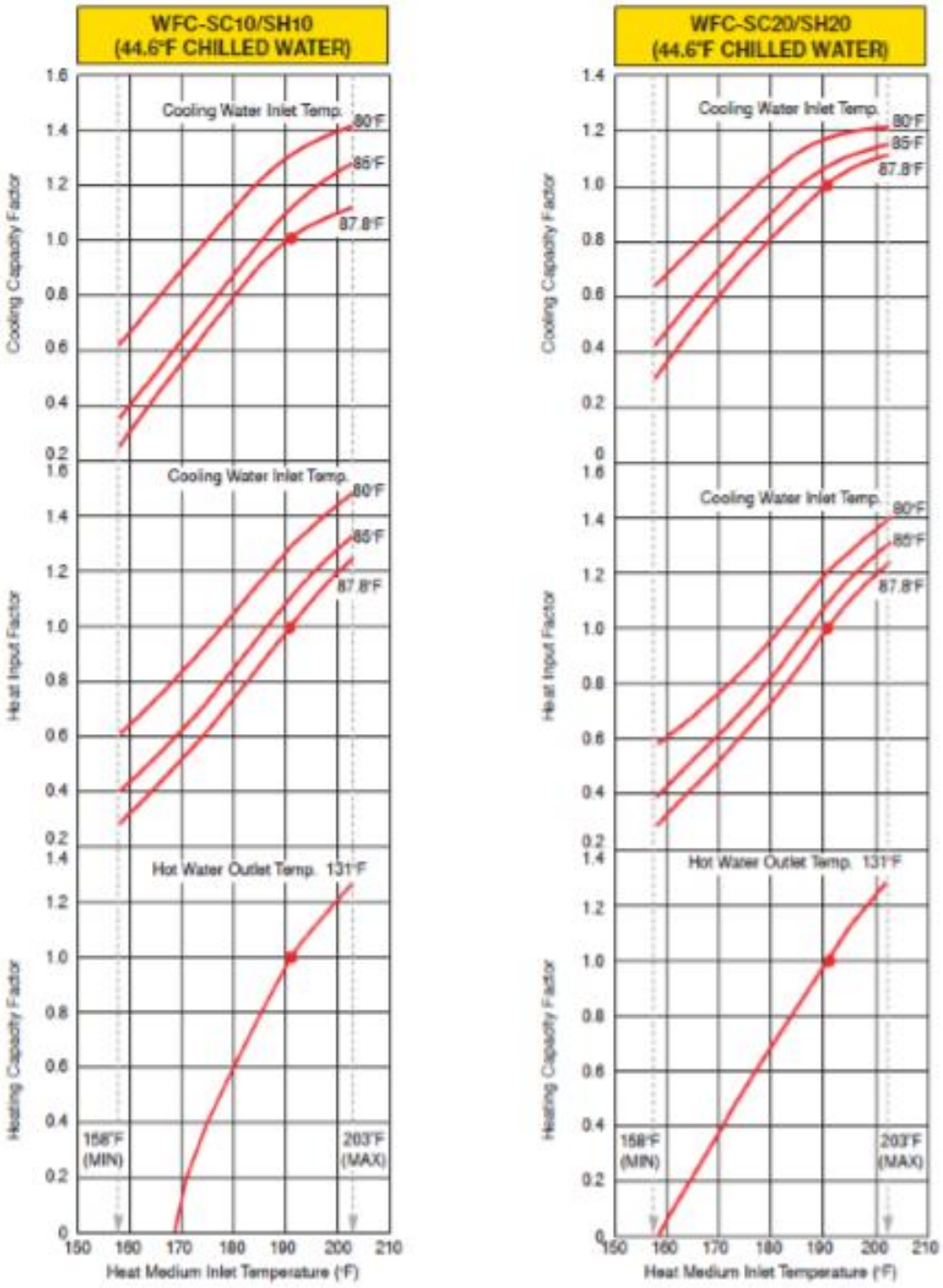

Figure B.1: Functioning Data of YAZAKI Absorption Chillers

ABSORPTION CHILLER HEAT BALANCE

HEAT IN = HEAT OUT

$$Q_g + Q_e = Q_c$$

Where, Q_g = Heat input to generator
Q_e = Cooling capacity
Q_c = Heat rejected to cooling tower

COOLING CAPACITY

$$Q_e = \text{CLG. CAP. FACTOR} \times \text{HM FLOW CORRECTION} \times \text{STD. CLG. CAPACITY}$$

HEAT INPUT (COOLING)

$$Q_g = \text{HEAT INPUT FACTOR} \times \text{HM FLOW CORRECTION} \times \text{STD. HEAT INPUT}$$

HEATING CAPACITY

$$Q_h = \text{HTG. CAP. FACTOR} \times \text{HM FLOW CORRECTION} \times \text{STD. HTG. CAPACITY}$$

Where, Q_h = Heating Capacity

HEAT INPUT (HEATING)

$$Q_g = \frac{\text{HEATING CAPACITY}}{\text{EFFICIENCY}} = \frac{Q_h}{0.97}$$

TEMPERATURE DIFFERENCE (°F)

$$\Delta T = \frac{\text{ADJUSTED CAPACITY OR HEAT INPUT (MBH)}}{0.5 \times \text{FLOW (gpm)}}$$

PRESS. DROP FOR NONSTANDARD FLOW (psi)

$$\Delta P = \text{STANDARD PRESS. DROP} \times \left(\frac{\text{NONSTANDARD FLOW}}{\text{STANDARD FLOW}}\right)^2$$

EXAMPLE 1.

Given design conditions:

Heat medium inlet temperature	195°F
Heat medium flow	114.1 gpm
Cooling water inlet temperature	85°F
Cooling water flow	242.5 gpm
Chilled water outlet temperature	44.6°F
Hot water outlet temperature	131°F
Chilled/hot water flow	72.6 gpm
Absorption chiller-heater model	WFC-SH30

Refer to Capacity Factor curves and Specifications for model WFC-SC30/SH30. Since 114.1 gpm is standard, the Heat Medium (HM) Flow Correction is 1.0.

1. AVAILABLE COOLING CAPACITY:

   Cooling Capacity Factor = 1.12

2. HEAT INPUT (COOLING):

   Heat Input Factor = 1.17
   Heat Medium Flow Correction = 1.0
   Standard Heat Input = 514.2 MBH
   Q_g = 1.17 x 1.0 x 514.2 = 601.6 MBH
   Heat Medium $\Delta T = \frac{601.6}{0.5 \times 114.1} = 10.5°F$
   Heat Medium ΔP = 8.8 psi (Standard)

3. HEAT REJECTED TO COOLING TOWER:

   $Q_c = Q_g + Q_e$ = 601.6 + 403.2 = 1004.8 MBH
   Cooling Water $\Delta T = \frac{1004.8}{0.5 \times 242.5} = 8.3°F$
   Cooling Water ΔP = 6.7 psi (Standard)

4. AVAILABLE HEATING CAPACITY:

   Heating Capacity Factor = 1.12
   Heat Medium Flow Correction = 1.0
   Standard Heating Capacity = 498.9 MBH
   Q_h = 1.12 x 1.0 x 498.9 = 558.8 MBH
   Hot Water $\Delta T = \frac{558.8}{0.5 \times 72.6} = 15.4°F$
   Hot Water ΔP = 10.1 psi (Standard)

5. HEAT INPUT (HEATING):

   $Q_g = \frac{Q_h}{0.97} = \frac{558.8}{0.97} = 576.1$ MBH

   Heat Medium $\Delta T = \frac{576.1}{0.5 \times 114.1} = 10.1°F$

   Heat Medium ΔP = 8.8 psi (Standard)

EXAMPLE 2.

Given design conditions:

Heat medium inlet temperature	203°F
Heat medium flow	57.0 gpm
Cooling water inlet temperature	85°F
Cooling water flow	242.5 gpm
Chilled water outlet temperature	44.6°F
Hot water outlet temperature	131°F
Chilled/hot water flow	72.6 gpm
Absorption chiller-heater model	WFC-SH30

Refer to Capacity Factor curves and Specifications for model WFC-SC30/SH30. Since 57.0 gpm is 50% of standard, the Heat Medium (HM) Flow Correction is 0.86.

1. AVAILABLE COOLING CAPACITY:

   Cooling Capacity Factor = 1.22

2. HEAT INPUT (COOLING):

Heat Input Factor = 1.35
Heat Medium Flow Correction = 0.86
Standard Heat Input = 514.2 MBH
Qg = 1.35 x 0.86 x 514.2 = 597.0 MBH

$$\text{Heat Medium } \Delta T = \frac{597.0}{0.5 \times 57.0} = 20.9°F$$

$$\text{Heat Medium } \Delta P = 8.8 \times \left(\frac{57.0}{114.1}\right)^2 = 2.2 \text{ psi}$$

3. HEAT REJECTED TO COOLING TOWER:

Qc = Qg + Qe = 597.0 + 377.7 = 974.7 MBH

$$\text{Cooling Water } \Delta T = \frac{974.7}{0.5 \times 242.5} = 8.0°F$$

Cooling Water ΔP = 6.7 psi (Standard)

4. AVAILABLE HEATING CAPACITY:

Heat Capacity Factor = 1.33
Heat Medium Flow Correction = 0.86
Standard Heating Capacity = 498.9 MBH
Qh = 1.33 x 0.86 x 498.9 = 570.6 MBH

$$\text{Hot Water } \Delta T = \frac{570.6}{0.5 \times 72.6} = 15.7°F$$

Hot Water ΔP = 10.1 psi (Standard)

5. HEAT INPUT (HEATING):

$$Qg = \frac{Qh}{0.97} = \frac{570.6}{0.97} = 588.2 \text{ MBH}$$

$$\text{Heat Medium } \Delta T = \frac{588.2}{0.5 \times 57.0} = 20.6°F$$

$$\text{Heat Medium } \Delta P = 8.8 \times \left(\frac{57.0}{114.1}\right)^2 = 2.2 \text{ psi}$$

Appendix C: Solar Collector Types via Detailed Properties

Technology Variant	CPC vacuum tube			Parabolic dish fixed	Parabolic dish tracking	Parabolic trough			Linear Fresnel
Specific thermal power (kW/m²)	0.60-0.65		0.3	0.21-0.31	0.34-0.74	0.50-0.56	0.22- 0.28	0.55-0.7	0.50-0.56
Location	China	Europe	India[a]	India	India[b,c]	Europe	Indiad	Mexico	Europe
Cost (USD/m²)	130	450-900	333	113-300	300-600	650	445	400-629	650-900
Cost (USD/kW)	200-220	690-1500	1133	365-1430	600-1760	1160-1300	1580-2040	570-1100	1160-1800

[a] PWC, 2013a, [b] PWC, 2013b, [c] PWC, 2013c, [d] PWC, 2013d

System Size	<0.07MW (<100m²)	0.07-0.35MW (100 -500m²)	0.35-0.7MW (500-1000m²)	> 0.7 MW (>1000m²)	Total
Number of Systems[a]	36	50	29	19	134
Installed Capacity, MW_{th}[b]	1.3	8.2	14.2	73.3	97
Installed Collector Area, m²	1796	11710	20227	104783	138515
Total investment Costs, USD[c]	932780	3259531	3710595	18036294	25939200
Average Investment Cost, USD/kW_{th}	1241	786	602	665	679

[a] Data based on AEE INTEC & PSE (2014) last accessed 07 Aug 2014

[b] Default value calculated by multiplying the gross collector area by 0.7 kWth/m² (IEA SHC, 2014a)

[c] Costs calculated for 67 projects in database with available data (1 EUR = 1,338 USD)

Table 8: C.1: Solar collectors via Detailed Properties.

Appendix D: Tool Function Parameters Obtained by TRNSYS

Table 9: D.1: Hot Water Storage Tank (Type 4a).

Parameter	value	Unit
Fixed inlet positions	1	default
Tank volume	3.0	m^3 (optimised)
Fluid specific heat	4.19	kJ/kg.K
Fluid density	1000	kg/m^3
Tank loss coefficient	0.6	$kJ/hr.m^2.K$ (Referenced)
Height of node-1	0.1	m
Height of node-2	0.1	m
Height of node-3	0.1	m
Height of node-4	0.1	m
Height of node-5	0.1	m
Height of node-6	0.1	m
Height of node-7	0.1	m
Height of node-8	0.1	m
Height of node-9	0.1	m
Height of node-10	0.1	m
Auxiliary heater mode	1	(off)
Node containing heating element 1	1	(top most element)
Node containing thermostat 1	1	(top most element)
Set point temperature for element 1	0	(off)
Dead band for heating element 1	5	delta °C (default)
Maximum heating rate of element 1	0	kJ/hr (off)
Node containing heating element 2	1	(top most element)
Node containing thermostat 2	1	(top most element)
Set point temperature for element 2	0	(off)
Dead band for heating element 2	5	delta °C (default)
Maximum heating rate of element 2	0	kJ/hr (off)
Not used (Flue UA)	0	W/K (not in use for storage tank)
Not used (T flue)	20	(not in use for storage tank)
Boiling point	100	°C
Hot-side temperature		°C (Collector Outlet water Temperature)
Hot-side flow rate	165	Kg/hr
Cold-side temperature		°C (Chiller Outlet water Temperature)
Cold-side flow rate	150	Kg/hr
Environment temperature		°C(Input from weather data)

Table 10: D.2: Single-Stage Absorption Chiller (Type 107).

Parameter	Value	Unit
Rated capacity	126000	kJ/hr (design)
Rated COP	0.7	- (Referenced)
Logical unit for S1 data file	40	(default)
Number of HW temperatures in S1 data file	5	(default)
Number of CW steps in S1 data file	3	(default)
Number of CHW set points in S1 data file	7	(default)
Number of load fractions in S1 data file	11	(default)
HW fluid specific heat	4.19	kJ/kg.K
CHW fluid specific heat	4.19	kJ/kg.K
CW fluid specific heat	4.19	kJ/kg.K
Auxiliary electrical power	220	kJ/hr (Referenced)
Chilled water inlet temperature	12.2	°C (chilled water outlet from Cooling coil)
Chilled water flow rate	5418	kg/hr (optimised)
Cooling water inlet temperature	22	°C (Cooled water outlet from cooling tower)
Cooling water flow rate	8190	kg/hr (optimised)
Hot water inlet temperature	98	°C (Hot water outlet from storage tank)
Hot water flow rate	4914	kg/hr (optimised)
CHW set point	6.667	°C (default)
Chiller control signal	1	(default)

Table 11: D.3: Cooling-Coil (Type 697).

Parameter	Value	Unit
Humidity mode	2	default -% relative humidity
Logical unit - water corrections	52	(default)
Number of water flow rates	3	-(default)
Number of water temperatures	3	-(default)
Logical unit - air flow corrections	53	-(default)
Number of air flows	7	-(default)
Logical unit - air temperature corrections	54	-(default)
Number of dry-bulb temperatures	7	-(default)
Number of wet-bulb temperatures	6	-(default)
Fluid density	1000	kg/m^3
Fluid specific heat	4.19	kJ/kg.K
Rated volumetric air flow rate	200	l/s (optimised)
Rated volumetric liquid flow rate	0.3	l/s (default)
Total cooling capacity	9000	kJ/hr (optimised)
Sensible cooling capacity	7150	kJ/hr (optimised)
Fluid inlet temperature	7	°C (Chilled water from chiller outlet)
Fluid flow rate	5418	kg/hr
Inlet air temperature		Fan outlet air
Inlet air flow rate	300	kg/hr (Fan outlet flow rate)
Inlet air pressure	1	atm (default)
Air-side pressure drop	0	atm (default)

Table 12: D.4: Parabolic Trough Solar Collector

Parameter	Value	Unit
Number in series	6	-
Collector area	30	m^2 (optimised value)
Fluid specific heat	4.19	kJ/kg.K
Efficiency mode	2	(optimised Value)
Flow rate at test conditions	3	$kg/hr.m^2$
Intercept efficiency	0.7	(default)
Negative of first order efficiency coefficient	9	$kJ/hr.m^2.K$ (Reference Model)
Negative of second order efficiency coefficient	0.03	$kJ/hr.m^2.K^2$(Reference Model)
Logical unit of file containing biaxial IAM data	60	(default)
Number of longitudinal angles for which IAMs are provided	5	(default)
Number of transverse angles for which IAMs are provided	5	(default)
Inlet temperature	°C (Storage tank cold side temperature)	
Inlet flow rate	165kg/hr	
Ambient temperature	Input from weather data	
Incident radiation		
Incident diffuse radiation		
Solar incidence angle		
Solar zenith angle		
Solar azimuth angle		
Collector slope	35	Degrees (optimised)
Collector azimuth	90	Degrees (optimised)